

On the Beta Prime Prior for Scale Parameters in High-Dimensional Bayesian Regression Models *

Ray Bai
Malay Ghosh †

University of Florida

June 17, 2022

Abstract

We study high-dimensional Bayesian linear regression with a general beta prime distribution for the scale parameter. To avoid misspecification of the hyperparameters and to enable our prior to adapt to *both* sparse and dense models, we propose a data-adaptive method for estimating the hyperparameters in the beta prime density. Our estimation of hyperparameters is based on maximization of marginal likelihood (MML), and we show how to incorporate our estimation procedure easily into our approximation of the posterior. Under our proposed empirical Bayes procedure, the MML estimates are never at risk of collapsing to zero. We also investigate the theoretical properties of our prior. We prove that careful selection of the hyperparameters leads to (near) minimax posterior contraction when $p \gg n$. As an aside, we also derive conditions for minimax posterior contraction under our prior for the sparse normal means problem. Finally, we demonstrate our prior's self-adaptivity and excellent finite sample performance through simulations and analysis of a gene expression data set.

*Keywords and phrases: empirical Bayes, high-dimensional data, linear regression, shrinkage estimation, scale mixtures of normal distributions, posterior contraction

†Malay Ghosh (email: ghoshm@ufl.edu) is Distinguished Professor, Department of Statistics, University of Florida. Ray Bai (email: raybai07@ufl.edu) is Graduate Student, Department of Statistics, University of Florida.

1 Introduction

1.1 Background

Consider the classical linear regression model,

$$\mathbf{y} = \mathbf{X}\boldsymbol{\beta} + \boldsymbol{\epsilon}, \quad (1.1)$$

where \mathbf{y} is an n -dimensional response vector, $\mathbf{X}_{n \times p} = [\mathbf{X}_1, \dots, \mathbf{X}_p]$ is a fixed regression matrix with n samples and p covariates, $\boldsymbol{\beta} = (\beta_1, \dots, \beta_p)'$ is a p -dimensional vector of unknown regression coefficients, and $\boldsymbol{\epsilon} \sim \mathcal{N}(\mathbf{0}, \sigma^2 \mathbf{I}_n)$, where σ^2 is the unknown variance. Throughout this paper, we assume that \mathbf{y} and \mathbf{X} have been centered at 0 so there is no intercept in our model.

In recent years, the high-dimensional setting when $p > n$ has received considerable attention. This scenario is now routinely encountered in areas as diverse as medicine, image reconstruction, astronomy, and finance, just to name a few. In the Bayesian framework, a popular method for estimating $\boldsymbol{\beta}$ in (1.1) when $p > n$ is to place scale-mixture shrinkage priors on the coefficients of interest and a prior on unknown variance, σ^2 . These priors take the form,

$$\begin{aligned} \beta_i | (\sigma^2, \omega_i^2) &\stackrel{i.i.d.}{\sim} \mathcal{N}(0, \sigma^2 \omega_i^2), i = 1, \dots, p, \\ \omega_i^2 &\stackrel{i.i.d.}{\sim} \pi(\omega_i^2), i = 1, \dots, p, \\ \sigma^2 &\sim \mu(\sigma^2), \end{aligned} \quad (1.2)$$

where $\pi : [0, \infty) \rightarrow [0, \infty)$ is a density on the positive reals. Priors of the form (1.2) have been considered by many authors, e.g., [24, 10, 19, 35, 4, 5, 28, 1, 20, 2].

Bayesian scale-mixture priors have been studied primarily under sparsity assumptions (e.g., [37, 39, 10, 34]). If sparse recovery of $\boldsymbol{\beta}$ is desired, the prior $\pi(\cdot)$ can be constructed so that it contains heavy mass around zero and heavy tails. This way, the posterior density $\pi(\boldsymbol{\beta}|\mathbf{Y})$ is also heavily concentrated around $\mathbf{0} \in \mathbb{R}^p$, while the heavy tails correctly identify and prevent overshrinkage of the true active covariates. In addition, these Bayesian methods provide a natural way to quantify uncertainty through the posterior density, $\pi(\boldsymbol{\beta}|\mathbf{y})$.

While sparsity is often a reasonable assumption, it is not always appropriate, nor is there any ironclad reason to believe that sparsity is the true phenomenon. As argued by Zou and Hastie [42], one of the limitations of many ℓ_1 regularization methods in frequentist approaches to large p , small n regression is their tendency to select at most n variables. Zou and Hastie

[42] introduced the elastic net to overcome the inability of the LASSO [36] to adapt to non-sparse situations.

In the Bayesian framework, there seems to be very little study of the appropriateness of scale-mixture priors (1.2) in dense settings. Ideally, we would like our priors on β to be able to adapt to *both* sparse and non-sparse situations. In this paper, we address this gap by showing that the use of a beta prime density as the scale parameter in (1.2) affords us the ability to adapt to different levels of sparsity or denseness. The beta prime density is given by

$$\pi(\omega_i^2) = \frac{\Gamma(a+b)}{\Gamma(a)\Gamma(b)} (\omega_i^2)^{a-1} (1+\omega_i^2)^{-a-b}. \quad (1.3)$$

In particular, setting $a = b = 0.5$ in (1.3) yields the half-Cauchy prior $\mathcal{C}^+(0, 1)$ for ω_i . In the normal means setting with $\mathbf{X} = \mathbf{I}$, $p = n$, and $\sigma^2 = 1$ in (1.1), Polson and Scott [28] conducted numerical experiments for different combinations of (a, b) in (1.3) and argued that the half-Cauchy prior should be a default prior for the top-level scale parameter in Bayesian hierarchical models. They reasoned that this is because the half-Cauchy prior “seems to occupy a sensible middle ground in terms of frequentist risk.” Polson and Scott [28] did not consider models more complicated than the normal means model.

In this paper, we study the empirical and theoretical properties of the general beta prime distribution (1.3) as a scale parameter for ω_i^2 in (1.2) for high-dimensional linear regression models. We call our model the normal-beta prime (NBP) model. Bai and Ghosh [3] previously studied the NBP model in the context of multiple hypothesis testing of normal means under sparsity assumptions. In this work, we extend the NBP prior to Bayesian linear regression models (1.1). We make the following contributions:

1. In our work, we allow the hyperparameters (a, b) in (1.3) to be data-dependent. We propose a data-adaptive method for estimating the hyperparameters (a, b) in the NBP model based on maximum marginal likelihood. Our empirical Bayes method enables the NBP prior to be self-adaptive, in the sense that it adapts to both sparse *and* dense situations. Moreover, our MML estimates of (a, b) are not at risk of collapsing to zero, an issue which is commonly faced by empirical Bayes procedures for other shrinkage priors.
2. For our theoretical investigation, we provide conditions on the hyperparameters (a, b) so that the posterior $\pi(\beta|\mathbf{Y})$ contracts at the (near) minimax contraction rate under the NBP prior when $p \gg n$. To our

knowledge, the theoretical study of optimal selection of hyperparameters (a, b) in the beta prime density (1.3) in linear regression models has not been previously undertaken, and our results lead to better understanding of the beta prime density as a scale parameter in Bayesian hierarchical models.

3. We also give conditions for minimax posterior contraction in the sparse normal means model and show that the optimal choices in this setting diverge sharply from those in the general high-dimensional regression setting. To our knowledge, no such contraction results have been previously established for the NBP prior.

The organization of this paper is as follows. In Section 2, we introduce the normal-beta prime (NBP) prior and demonstrate how different choices of the hyperparameters lead to either sparse or dense recovery of β in (1.1). In Section 3, we introduce a maximum marginal likelihood approach to estimating the hyperparameters in the NBP prior and show how our estimate can be easily incorporated into both Gibbs sampling and variational inference schemes. In Section 4, we provide conditions for (near) minimax posterior contraction for high-dimensional ($p \gg n$) regression. We also establish minimax posterior contraction results for the sparse normal means problem and show how these results fundamentally differ from those in regression under general design. In Section 5, we present simulation results which demonstrate that the NBP prior has excellent performance for both estimation and variable selection in finite samples. Finally, in Section 6, we utilize the NBP prior to analyze a gene expression data set.

1.2 Notation

We use the following notations for the rest of the paper. Let $\{a_n\}$ and $\{b_n\}$ be two non-negative sequences of real numbers indexed by n , where $b_n \neq 0$ for sufficiently large n . We write $a_n \asymp b_n$ to denote $0 < \liminf_{n \rightarrow \infty} a_n/b_n \leq \limsup_{n \rightarrow \infty} a_n/b_n < \infty$. If $\lim_{n \rightarrow \infty} a_n/b_n = 1$, we write it as $a_n \sim b_n$. If $\lim_{n \rightarrow \infty} a_n/b_n = 0$, we write $a_n = o(b_n)$ or $a_n \prec b_n$. We use $a_n \lesssim b_n$ or $a_n = O(b_n)$ to denote that for sufficiently large n , there exists a constant $C > 0$ independent of n such that $a_n \leq Cb_n$ respectively.

For a vector $\mathbf{v} \in \mathbb{R}^p$, we let $\|\mathbf{v}\|_0 := \sum_{i=1}^p \mathbf{1}(v_i \neq 0)$, $\|\mathbf{v}\|_1 := \sum_{i=1}^p |v_i|$, and $\|\mathbf{v}\|_2 := \sqrt{\sum_{i=1}^p v_i^2}$ denote the ℓ_0 , ℓ_1 , and ℓ_2 norms respectively. For a set \mathcal{A} , we denote its cardinality as $|\mathcal{A}|$.

2 The Normal-Beta Prime (NBP) Model

Suppose that we place a normal-scale mixture prior with the beta prime density (1.3) as the scale parameter for each of the individual coefficients in $\boldsymbol{\beta} = (\beta_1, \dots, \beta_p)$ and the usual inverse gamma prior $\mathcal{IG}(c, d)$ prior on σ^2 , where $c, d > 0$. Letting $\beta'(a, b)$ denote the beta prime distribution (1.3) with hyperparameters $a > 0, b > 0$, we specify our Bayesian hierarchy as follows:

$$\begin{aligned} \beta_i | \omega_i^2, \sigma^2 &\stackrel{i.i.d.}{\sim} \mathcal{N}(0, \sigma^2 \omega_i^2), i = 1, \dots, p, \\ \omega_i^2 &\stackrel{i.i.d.}{\sim} \beta'(a, b), i = 1, \dots, p, \\ \sigma^2 &\sim \mathcal{IG}(c, d), \end{aligned} \tag{2.1}$$

For our model (2.1), we can choose c and d appropriately in order to make the prior on σ^2 relatively noninfluential and noninformative (e.g., a good default choice is $c = d = 10^{-5}$). The most critical hyperparameter choices for our model are (a, b) . As Polson and Scott [28] describe, the parameter a controls the heaviness of the tails in the marginal density $\pi(\beta_i | \sigma^2)$, while b controls the amount of mass around zero. In fact, if we set $b \in (0, 1/2]$, we have the following proposition:

Proposition 2.1. *Suppose that we endow $(\boldsymbol{\beta}, \sigma^2)$ with the priors in (2.1). Then the marginal distribution, $\pi(\beta_i | \sigma^2), i = 1, \dots, p$, is unbounded with a singularity at zero for any $0 < b \leq 1/2$.*

Proof. See Proposition 1 in Bai and Ghosh [3]. □

Proposition 2.1 implies that in order to facilitate sparse recovery of $\boldsymbol{\beta}$, we should set b to be a small value. This would force the NBP prior to place most of its mass near zero, and thus, the posterior $\pi(\boldsymbol{\beta} | \mathbf{y})$ would also be concentrated near $\mathbf{0} \in \mathbb{R}^p$. As we demonstrate in Section 4, setting b to be a small number dependent upon both sample size and predictor dimension is the key ingredient in obtaining optimal posterior contraction rates under sparsity assumptions.

On the other hand, if we desire a more dense model, then setting a larger b results in a more diffuse prior. So there would be less shrinkage of individual covariates in the posterior distribution. Figure 1 plots the marginal density, $\pi(\beta | \sigma^2)$, for a single β , where we set $\sigma^2 = 1$ for illustration. We see that with $b = 0.1$, the marginal density contains a singularity at zero, and the probability mass is heavily concentrated near zero. However, when $b = 2$, the marginal density does not contain a pole at zero, and the tails are significantly heavier. Clearly, b is the main parameter which controls the sparsity in our estimate of $\boldsymbol{\beta}$.

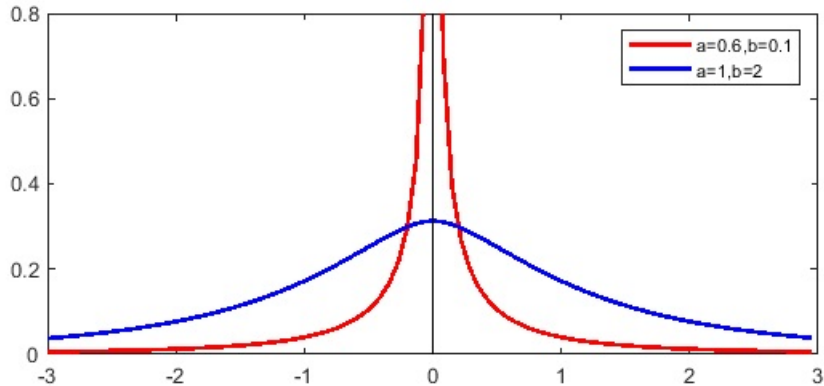


Figure 1: The marginal densities of the NBP prior, $\pi(\beta|\sigma^2)$, with $\sigma^2 = 1$. A smaller b leads to a pole at zero and most of the mass near zero, whereas a large b removes the singularity and leads to a more diffuse prior with heavier tails.

Figure 1 also shows that our prior is very sensitive to misspecification of hyperparameters. If we believe the true model is sparse with a few large signal values, then there is possibly not much loss in fixing b *a priori* to be a very small value. However, if the true model is actually dense, then setting b to be too small would both overestimate the true sparsity level and overshrink small signal values. Ideally, we would like the NBP model to *learn* the true sparsity from the data.

3 Empirical Bayes Estimation of Hyperparameters

We propose an EM algorithm to obtain maximum marginal likelihood (MML) estimates of (a, b) , which enables our model to be self-adaptive and learn the underlying sparsity (or non-sparsity). Our algorithm can be easily incorporated into Gibbs sampling or variational inference algorithms. In Appendix A, we provide the complete technical details for the Gibbs sampling and mean field variational Bayes (MFVB) algorithms. The EM algorithm we describe in this section can be easily embedded into either approach. Furthermore, the EM approach for estimating (a, b) avoids collapse to zero.

To construct the EM algorithm, first note that because the beta prime density can be rewritten as a product of an independent inverse gamma and gamma densities, we may reparametrize (2.1) as

$$\begin{aligned}
\beta_i | (\omega_i^2, \lambda_i^2 \xi_i^2) &\stackrel{i.i.d.}{\sim} \mathcal{N}(0, \sigma^2 \lambda_i^2 \xi_i^2), i = 1, \dots, p, \\
\lambda_i^2 &\stackrel{i.i.d.}{\sim} \mathcal{IG}(a, 1), i = 1, \dots, p, \\
\xi_i^2 &\stackrel{i.i.d.}{\sim} \mathcal{G}(b, 1), i = 1, \dots, p, \\
\sigma^2 &\sim \mathcal{IG}(c, d).
\end{aligned} \tag{3.1}$$

The logarithm of the joint posterior under the reparametrized NBP prior (3.1) is given by

$$\begin{aligned}
& - \left(\frac{n+p}{2} \right) \log(2\pi) - \left(\frac{n+p}{2} + c + 1 \right) \ln(\sigma^2) - \frac{1}{2\sigma^2} \|\mathbf{y} - \mathbf{X}\boldsymbol{\beta}\|_2^2 \\
& - \sum_{i=1}^p \frac{\beta_i^2}{2\lambda_i^2 \xi_i^2 \sigma^2} - p \ln(\Gamma(a)) - \left(a + \frac{3}{2} \right) \sum_{i=1}^p \ln(\lambda_i^2) - \sum_{i=1}^p \frac{1}{\lambda_i^2} \\
& - p \ln(\Gamma(b)) + \left(b - \frac{3}{2} \right) \sum_{i=1}^p \ln(\xi_i^2) - \sum_{i=1}^p \xi_i^2 + c \ln(d) - \ln(\Gamma(c)) - \frac{d}{\sigma^2}.
\end{aligned} \tag{3.2}$$

Thus, at the k th iteration the EM algorithm, the conditional log-likelihood on $\nu^{(k-1)} = (a^{(k-1)}, b^{(k-1)})$ and \mathbf{y} in the E-step is given by

$$\begin{aligned}
Q(\nu | \nu^{(k-1)}) &= -p \ln(\Gamma(a)) - a \sum_{i=1}^p \mathbb{E}_{a^{(k-1)}} [\ln(\lambda_i^2) | \mathbf{y}] - p \ln(\Gamma(b)) \\
& + b \sum_{i=1}^p \mathbb{E}_{b^{(k-1)}} [\ln(\xi_i^2) | \mathbf{y}] + \text{terms not involving } a \text{ or } b.
\end{aligned} \tag{3.3}$$

The M-step maximizes $Q(\nu | \nu^{(k-1)})$ over $\nu = (a, b)$ to produce the next estimate $\nu^{(k)} = (a^{(k)}, b^{(k)})$. That is, we must find (a, b) such that

$$\begin{aligned}
\frac{\partial Q}{\partial a} &= -p\psi(a) - \sum_{i=1}^p \mathbb{E}_{a^{(k-1)}} [\ln(\lambda_i^2) | \mathbf{y}] = 0, \\
\frac{\partial Q}{\partial b} &= -p\psi(b) + \sum_{i=1}^p \mathbb{E}_{b^{(k-1)}} [\ln(\xi_i^2) | \mathbf{y}] = 0, \\
a &> 0, b > 0,
\end{aligned} \tag{3.4}$$

where $\psi(x) = d/dx (\Gamma(x))$ denotes the digamma function. We can solve for (a, b) in (3.4) numerically by using a fast root-finding algorithm such as Newton's algorithm. The summands, $\mathbb{E}_{a^{(k-1)}} [\ln(\lambda_i^2) | \mathbf{y}]$ and $\mathbb{E}_{b^{(k-1)}} [\ln(\xi_i^2) | \mathbf{y}]$, $i = 1, \dots, p$, in (3.4) can be estimated from either the mean of M Gibbs samples based on $\nu^{(k-1)}$, for sufficiently large M (as in [11]), or from the

$(k-1)$ st iteration of the MFVB algorithm (as in [23]). In particular, Casella [11] proved that the EM/Gibbs sampling algorithm is statistically valid, in the sense that the iterates $\nu^{(k)}$ approach the true MML estimator $\hat{\nu} = (\hat{a}, \hat{b})$ and that the EM/Gibbs algorithm leads to consistent estimation of the posterior $\pi(\boldsymbol{\beta}|\hat{\nu}, \mathbf{y})$.

Theorem 3.1. *At the k th iteration of the EM algorithm, there exists a unique solution $\nu^{(k)} = (a^{(k)}, b^{(k)})$, which maximizes (3.3) in the M -step. Moreover, $a^{(k)} > 0$, $b^{(k)} > 0$ at the k th iteration.*

Proof. See Appendix A. □

Theorem 3.1 ensures that under our setup, we will not encounter the issue of the sparsity parameter b (or the parameter a) collapsing to zero. Empirical Bayes estimates of zero are a major concern for MML approaches for estimating hyperparameters in Bayesian linear regression models. For example, in g -priors,

$$\boldsymbol{\beta}|\sigma^2 \sim \mathcal{N}_p\left(\boldsymbol{\gamma}, g\sigma^2(\mathbf{X}^\top \mathbf{X})^{-1}\right),$$

George and Foster [15] showed that the MML estimate of the parameter g could equal zero. In global-local shrinkage priors of the form,

$$\beta_i | (\lambda_i^2, \sigma^2) \sim \mathcal{N}(0, \sigma^2 \tau^2 \lambda_i^2), \quad \lambda_i^2 \sim \pi(\lambda_i^2), \quad i = 1, \dots, p,$$

the global parameter τ is also at risk of being estimated as zero [27, 33, 9]. Some authors, e.g. [27, 12, 9], have therefore cautioned against the use of empirical Bayes estimation of hyperparameters in continuous shrinkage priors. However, with the NBP prior, we can easily incorporate a data-adaptive procedure for estimating the hyperparameters while avoiding this potential pitfall.

For g -priors and global-local shrinkage priors, placing priors on g or τ with strictly positive support can help to avoid the issue of collapse to zero. However, this hierarchical Bayes approach still does not quite mitigate the problem of misspecification of hyperparameters (since these would still need to be specified in the additional priors), nor does it necessarily afford these models the ability to adapt to dense settings in the same ways that the empirical Bayes variant of the NBP prior does.

3.1 Illustration of the NBP Prior’s Self-Adaptivity

In this section, we illustrate the self-adaptivity of the NBP prior. We consider two settings: one sparse ($n = 50$, $p = 100$, 10 nonzero covariates) and

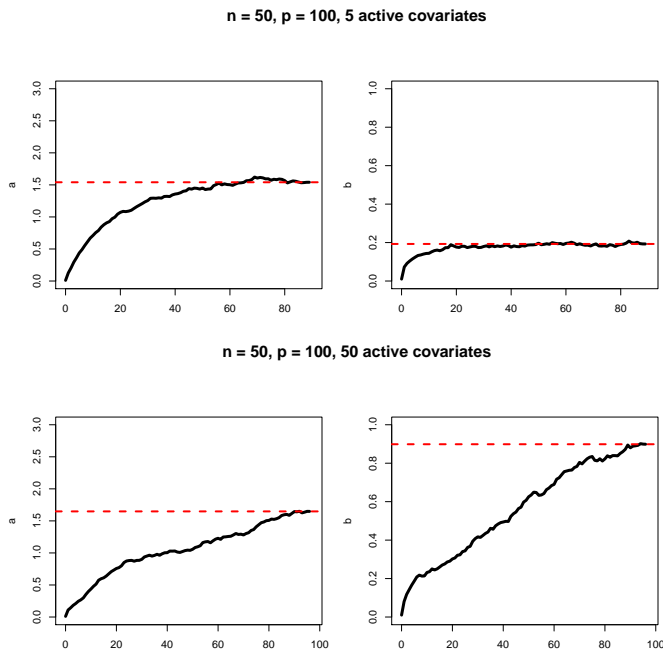


Figure 2: Paths of the Monte Carlo/EM algorithm for estimating the MML estimators of a and b for one sparse case and one dense case. The dashed red line indicates the final MML estimate at convergence. We see that our algorithm learns the true sparsity level of the underlying model (with a smaller estimate of b when the model is truly sparse, and a larger estimate of b when the model is truly dense).

one dense ($n = 50$, $p = 100$, and 50 active covariates), where the active covariates are drawn from $\mathcal{U}([-2, -0.5] \cup [0.5, 2])$. Our simulations come from experiments 1 and 4 in Section 5. Section 5 describes the exact model generating mechanisms for our simulations. For our examples, we initialize our EM algorithm with $(a^{(0)}, b^{(0)}) = (0.01, 0.01)$ and then implement the EM/Gibbs algorithm introduced in Section 3 for finding the MML estimates of the parameters (a, b) , which we denote as (\hat{a}, \hat{b}) .

In Figure 2, we plot the iterations from two runs of the EM algorithm. The algorithm terminates at iteration k when the square of the ℓ_2 distance between $(a^{(k-1)}, b^{(k-1)})$ and $(a^{(k)}, b^{(k)})$ reaches below 10^{-6} . We then set $(\hat{a}, \hat{b}) = (a^{(k)}, b^{(k)})$. The top panel in Figure 2 plots the paths for a and b from a sparse model with 5 active predictors, and the bottom panel plots the paths for a and b from a dense model with 50 active predictors. In the sparse case, the final MML estimate of b is $\hat{b} = 0.193$. In the dense case, the final MML estimate of b is $\hat{b} = 0.899$.

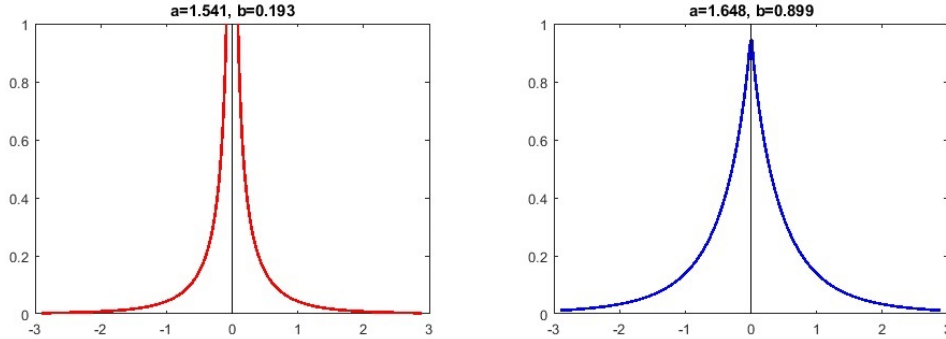


Figure 3: The marginal densities of the NBP prior, $\pi(\beta|a, b, \sigma^2)$, with different MML estimates of (a, b) . The left panel depicts the marginal density under the sparse setting ($a = 1.541, b = 0.193$), and the right panel depicts the marginal density under the dense setting ($a = 1.648, b = 0.899$).

Figure 3 shows the NBP’s marginal density, $\pi(\beta|\hat{a}, \hat{b}, \sigma^2)$, for a single coefficient β using the MML estimates of (a, b) obtained in sparse and the dense settings respectively. For the purpose of illustration, we have fixed $\sigma^2 = 1$. We see that in the sparse setting (five active predictors, $(\hat{a}, \hat{b}) = (1.541, 0.193)$), the marginal density for β contains a singularity at zero, *and* most of the probability mass is around zero. After the final MML estimates (\hat{a}, \hat{b}) have been obtained from the EM algorithm, we can generate a final sample of the Gibbs sampler or the variational inference algorithm to estimate the posterior $\pi(\beta|\hat{a}, \hat{b}, \mathbf{y})$. We thus recover a sparse model for $\pi(\beta|\mathbf{y})$ under these MML hyperparameters. Meanwhile, in the dense setting (50 active predictors, $(\hat{a}, \hat{b}) = (1.648, 0.899)$), the marginal density for β does not contain a pole and more mass is placed in neighborhoods away from zero, meaning that our model will be more dense.

Figures 2 and 3 illustrate that in both the sparse and dense cases, the EM algorithm was able to correctly learn the true sparsity (or non-sparsity) from the data and incorporate this into its estimates of the hyperparameters. In short, the NBP prior with MML estimates of its shape parameters has several highly desirable properties: 1) it is self-adaptive and can be useful in modeling *both* sparse and dense scenarios, 2) its empirical Bayes estimates for its hyperparameters are never at risk of collapsing to zero, and 3) it avoids the delicate issue of misspecification of hyperparameters.

4 Posterior Contraction Rates Under the NBP Prior

For our theoretical analysis of the NBP prior, we shall be principally concerned with the case when p diverges to infinity as sample size n grows. For the remainder of this section, we rewrite p as p_n to emphasize its dependence on n . We work under the frequentist assumption that there is a true data-generating model, i.e.,

$$\mathbf{y}_n = \mathbf{X}_n \boldsymbol{\beta}_0 + \boldsymbol{\epsilon}_n, \quad (4.1)$$

where $\boldsymbol{\epsilon}_n \sim \mathcal{N}(\mathbf{0}, \sigma_0^2 \mathbf{I}_n)$ and σ_0^2 is a fixed noise parameter.

4.1 Contraction Results for High-Dimensional Regression

4.1.1 Preliminaries

Let $s = \|\boldsymbol{\beta}_0\|_0$ denote the size of the true model, and suppose that $s = o(n/\log p_n)$. Under (4.1) and appropriate regularity conditions, Raskutti et al. [29] showed that the minimax estimation rate for any point estimator $\hat{\boldsymbol{\beta}}$ of $\boldsymbol{\beta}_0$ under ℓ_2 error loss is $\sqrt{s \log(p_n/s)/n}$. Many frequentist point estimators such as the LASSO [36] and the Dantzig [8] estimators have been shown to attain the *near*-minimax rate of $\sqrt{s \log p_n/n}$ under ℓ_2 error loss.

In the Bayesian paradigm, on the other hand, we are interested in the rate at which the *entire* posterior distribution contracts around the true $\boldsymbol{\beta}_0$. Letting \mathbb{P}_0 denote the probability measure underlying (4.1) and $\Pi(\boldsymbol{\beta}|\mathbf{y}_n)$ denote the posterior distribution of $\boldsymbol{\beta}$, our aim is to find a positive, nonincreasing sequence r_n such that

$$\Pi(\boldsymbol{\beta} : \|\boldsymbol{\beta} - \boldsymbol{\beta}_0\| \geq M r_n | \mathbf{y}_n) \rightarrow 0 \text{ a.s. } \mathbb{P}_0 \text{ as } n \rightarrow \infty,$$

for some constant $M > 0$. The frequentist minimax convergence rate is a useful benchmark for the speed of contraction r_n , since the posterior cannot contract faster than the minimax rate [16]. Moreover, if the posterior contracts at the (near) minimax rate, then the posterior credible sets also provide a more realistic measure of uncertainty quantification [39].

Additionally, we are interested in posterior *compressibility* [7], which enables us to quantify how well the NBP posterior captures the true sparsity level s . Since the NBP prior is absolutely continuous, it assigns zero mass to exactly sparse vectors. To approximate the model size for the NBP model, we use the following generalized notion of sparsity [30, 31, 7]. Letting δ be some positive constant (to be specified later), we define the generalized

inclusion indicator and generalized dimensionality, respectively, as

$$\gamma_\delta(\boldsymbol{\beta}) = I(|\boldsymbol{\beta}/\sigma| > \delta) \text{ and } |\gamma_\delta(\boldsymbol{\beta})| = \sum_{i=1}^{p_n} \gamma_\delta(\beta_i). \quad (4.2)$$

The generalized dimensionality counts the number of covariates in $\boldsymbol{\beta}/\sigma$ that fall outside the interval $[-\delta, +\delta]$. With appropriate choice of δ , the prior is said to have the posterior compressibility property if the probability that $|\gamma_\delta(\boldsymbol{\beta})|$ asymptotically exceeds a constant multiple of the true sparsity level s tends to 0 as $n \rightarrow \infty$, i.e.

$$\Pi(\boldsymbol{\beta} : |\gamma_\delta(\boldsymbol{\beta})| \geq As|\mathbf{y}_n) \rightarrow 0 \text{ a.s. } \mathbb{P}_0 \text{ as } n \rightarrow \infty,$$

for some constant $A > 0$.

4.1.2 Near-Minimax Posterior Contraction Under the NBP Prior

Under model (4.1), Song and Liang [34] recently derived sufficient conditions for priors of the form,

$$\pi(\boldsymbol{\beta}|\sigma^2) = \prod_{i=1}^p [g(\beta_i/\sigma)/\sigma], \quad \sigma^2 \sim \mathcal{IG}(c, d), \quad (4.3)$$

under which the posterior for $\boldsymbol{\beta}$ contracts around $\boldsymbol{\beta}_0$ at near-minimax rates with respect to ℓ_2 , ℓ_1 , and prediction error loss, and under which these priors possess the posterior compressibility property. Roughly speaking, these conditions require that the density $g(\cdot)$ puts enough mass inside a shrinking interval around zero, and that for true nonzero coefficients β_{0i} , $g(\beta_{0i}/\sigma)$ is sufficiently large. This latter condition is equivalent to requiring that tails of g be sufficiently heavy.

Using these general conditions, Song and Liang [34] provided sufficient conditions for near-minimax posterior contraction and posterior compressibility for both spike-and-slab priors and priors of the form,

$$\beta_i|\omega_i^2, \sigma^2 \stackrel{i.i.d.}{\sim} \mathcal{N}(0, \omega_i^2\sigma^2), \quad \omega_i^2 \stackrel{i.i.d.}{\sim} \pi_{\tau_n}(\omega_i^2), i = 1, \dots, p_n, \quad (4.4)$$

where $\pi_{\tau_n}(\omega_i^2)$ is a polynomial-tailed prior of the form $\pi_{\tau_n}(\cdot) = \pi(\cdot/\tau_n)/\tau_n$ and $\tau_n > 0$ is a scaling hyperparameter. Priors of this form are also known as global-local shrinkage priors. See, e.g., [10, 20, 7, 27].

The NBP prior is of the form (4.3) but it is *not* of the form (4.4). Therefore, in order to verify that the NBP posterior contracts at near-minimax

rates and that it possesses posterior compressibility, a separate proof verifying the conditions of Song and Liang [34] is required. In fact, as Theorem 4.1 shows, provided that b decays to zero at an appropriate rate (which depends on both n and p_n) as $n \rightarrow \infty$, the NBP also shares these optimal theoretical properties. For the remainder of this section, we denote b as b_n to emphasize its dependence on n (and p_n).

We first introduce the following set of regularity conditions, which come from [34] and which are fairly standard in the high-dimensional literature. As before, s denotes the size of the true model, while $\lambda_{\min}(\mathbf{A})$ denotes the minimum eigenvalue of a symmetric matrix \mathbf{A} .

Regularity conditions

- (A1) All the covariates are uniformly bounded. For simplicity, we assume they are all bounded by 1.
- (A2) $p_n \gg n$.
- (A3) Let ξ denote a set of indices where $\xi \subset \{1, \dots, p_n\}$, and let \mathbf{X}_ξ denote the submatrix of \mathbf{X}_n that contains the columns with indices in ξ . There exists some integer \bar{p} (depending on n and p_n) and fixed constant t_0 such that $\bar{p} \succ s$ and $\lambda_{\min}(\mathbf{X}_\xi^\top \mathbf{X}_\xi) \geq nt_0$ for any model of size $|\xi| \leq \bar{p}$.
- (A4) $s := s_n = o(n/\log p_n)$.
- (A5) $\max_j \{|\beta_{0j}/\sigma|\} \leq \gamma_3 E_n$ for some $\gamma_3 \in (0, 1)$, and E_n is nondecreasing with respect to n .

Assumption (A3) is a minimum restricted eigenvalue (RE) condition which ensures that $\mathbf{X}^\top \mathbf{X}$ is locally invertible over sparse sets. When $p_n \geq O(n)$, minimum RE conditions are routinely imposed to render β_0 estimable. Assumption (A4) restricts the growth of s , and (A5) constrains the size of the signals in β_0 to be $O(E_n)$ for some nondecreasing sequence E_n (the specific rate which may differ for different priors).

Under the above regularity conditions, we are now ready to state our main theorem which shows that in high-dimensional regression, the posterior distribution under the NBP prior (2.1) contracts at near-minimax rates and achieves posterior compressibility.

Theorem 4.1. *Assume that Assumptions (A1)-(A5) hold, with $\log(E_n) = O(\log p_n)$ for Assumption (A5). Let $r_n = M\sqrt{s \log p_n/n}$ for some fixed constant $M > 0$, and let $k_n \asymp (\sqrt{s \log p_n/n})/p_n$. Suppose that we place the*

NBP prior (2.1) on $(\boldsymbol{\beta}, \sigma^2)$, with $a \in (1/2, \infty)$ and $b_n \lesssim p_n^{-(1+u)}$, where $u > 0$. Then under (4.1), the following hold:

$$\Pi(\boldsymbol{\beta} : \|\boldsymbol{\beta} - \boldsymbol{\beta}_0\|_2 \geq c_1 \sigma r_n | \mathbf{y}_n) \rightarrow 0 \text{ a.s. } \mathbb{P}_0 \text{ as } n \rightarrow \infty, \quad (4.5)$$

$$\Pi(\boldsymbol{\beta} : \|\boldsymbol{\beta} - \boldsymbol{\beta}_0\|_1 \geq c_1 \sigma \sqrt{s r_n} | \mathbf{y}_n) \rightarrow 0 \text{ a.s. } \mathbb{P}_0 \text{ as } n \rightarrow \infty, \quad (4.6)$$

$$\Pi(\boldsymbol{\beta} : \|\mathbf{X}\boldsymbol{\beta} - \mathbf{X}\boldsymbol{\beta}_0\|_2 \geq c_0 \sigma \sqrt{n r_n} | \mathbf{Y}_n) \rightarrow 0 \text{ a.s. } \mathbb{P}_0 \text{ as } n \rightarrow \infty, \quad (4.7)$$

$$\Pi(\boldsymbol{\beta} : |\gamma_{k_n}(\boldsymbol{\beta})| \geq \tilde{p} | \mathbf{y}_n) \rightarrow 0 \text{ a.s. } \mathbb{P}_0 \text{ as } n \rightarrow \infty, \quad (4.8)$$

where $c_0 > 0, c_1 > 0$, $\gamma_{k_n}(\beta_i) = I(|\beta_i/\sigma| > k_n)$, and $\tilde{p} \asymp s$.

Proof. See Appendix B. □

In Theorem 4.1, (4.5)-(4.7) show that with appropriate choices of (a, b_n) , the NBP prior's posterior contraction rates under ℓ_2 , ℓ_1 , and prediction error loss respectively are the familiar near-optimal rates of $O(\sqrt{s \log p_n/n})$, $O(s\sqrt{\log p_n/n})$, and $O(\sqrt{s \log p_n})$ respectively. Moreover, by setting $\delta = k_n \asymp (\sqrt{s \log p_n/n})/p_n$ in our generalized inclusion indicator (4.2), (4.8) also shows that the probability that the NBP posterior's generalized dimension size is a constant multiple larger than s asymptotically vanishes.

4.2 Sparse Normal Means Problem

We also consider the sparse normal means model,

$$\mathbf{y}_n = \boldsymbol{\beta}_0 + \boldsymbol{\epsilon}_n, \quad (4.9)$$

where $\boldsymbol{\epsilon}_n \sim \mathcal{N}(\mathbf{0}, \mathbf{I}_n)$. This model is obviously a special case of (4.1), with $n = p$, $\mathbf{X}_n = \mathbf{I}_n$ and $\sigma^2 = 1$. Model (4.9) has arisen as an important test case for studying sparsity methods and has found some applications (e.g., image processing and wavelet analysis [22]). In [34], it was remarked that results for the normal means model do not generalize to general regression settings, and we confirm this for the NBP prior in this section.

Suppose we observe \mathbf{y}_n from (4.9). Let $\ell_0[q_n]$ denote the subset of \mathbb{R}^n given by

$$\ell_0[q_n] = \{\boldsymbol{\beta} \in \mathbb{R}^n : \#\{1 \leq i \leq n : \beta_i \neq 0\} \leq q_n\}. \quad (4.10)$$

If $\boldsymbol{\beta}_0 \in \ell_0[q_n]$ with $q_n = o(n)$ as $n \rightarrow \infty$, we say that $\boldsymbol{\beta}_0$ is sparse in the ‘‘nearly black sense’’ [13]. In the class of ‘‘nearly black’’ vectors $\boldsymbol{\beta}_0$, the minimax posterior contraction rate under squared error loss is $q_n \log(n/q_n)$ [13].

Many normal scale-mixture shrinkage priors of the form,

$$\beta_i | \lambda_i^2 \sim \mathcal{N}(0, \lambda_i^2), \quad \lambda_i^2 \sim \pi(\lambda_i^2), \quad i = 1, \dots, n, \quad (4.11)$$

are known to attain minimax posterior contraction under (4.9). When the priors $\pi(\lambda_i^2)$ in (4.11) are *a priori* independent, van der Pas et al. [37] provided conditions on $\pi(\lambda_i^2)$ under which the posterior contracts at rate $q_n \log(n/q_n)$. They claimed that their conditions are nearly sharp, but we are unable to verify one of their conditions for the NBP prior. One of the conditions required by [37] is as follows:

- Let $\pi_n(\cdot)$ be the density of the scale parameter λ_i^2 in (4.11), which depends on n . Suppose that there is a constant $c > 0$ such that

$$\int_0^1 \pi_n(u) du \geq c. \quad (4.12)$$

While for a *fixed* shape parameter b , it is possible to satisfy (4.12) for the NBP prior, this is not the case when b decays to zero. Suppose we have the NBP model with shape parameters (a, b_n) where $a \in (1/2, \infty)$ and $b_n = o(1)$, i.e.

$$\begin{aligned} \beta_i | \omega_i^2 &\stackrel{i.i.d.}{\sim} \mathcal{N}(0, \omega_i^2), \quad i = 1, \dots, n, \\ \omega_i^2 &\stackrel{i.i.d.}{\sim} \beta'(a, b_n), \quad i = 1, \dots, n. \end{aligned} \quad (4.13)$$

We call this variant (4.13) of the NBP model as the NBP_n prior. The next proposition shows that for the NBP_n prior, the integral of the beta prime prior evaluated on the interval $[0, 1]$ is always of the order $O(b_n)$. Previously, Bai and Ghosh [3] showed that this integral was of order $O(b_n^{1/2})$. It turns out that we are able to sharpen our bound even further.

Proposition 4.1. *Let $\pi_n(u)$ be the beta prime prior (1.3) with shape parameters (a, b_n) . For any $a \in (1/2, \infty)$ and $b_n \in (0, 1)$ such that $b_n \rightarrow 0$ as $n \rightarrow \infty$,*

$$\int_0^1 \pi_n(u) du = O(b_n).$$

Proof. See Appendix B. □

Since $b_n \rightarrow 0$ as $n \rightarrow \infty$, Proposition 4.1 implies that $\int_0^1 \pi_n(u) du \rightarrow 0$ as $n \rightarrow \infty$, i.e. for any $c' > 0$, $\int_0^1 \pi_n(u) du \leq c'$ for sufficiently large n . Therefore, condition (4.12) is not satisfied for the NBP_n prior. Although it does not seem as though the conditions of [37] hold for our prior, the next theorem establishes that the NBP_n model (4.13) nevertheless *does* obtain the minimax posterior contraction rate with suitable shape parameters.

Theorem 4.2. *Suppose that we observe \mathbf{y}_n from (4.9) and that $q_n = o(n)$. Suppose we place the NBP $_n$ prior (4.13) on β with $a \in (1/2, \infty)$ and $b_n = (q_n/n)^\alpha, \alpha \geq 1$. Then the following hold:*

$$\sup_{\beta_0 \in \ell_0[q_n]} \mathbb{E}_{\beta_0} \Pi \left(\beta : \|\beta - \beta_0\|_2^2 > M_n q_n \log \left(\frac{n}{q_n} \right) \middle| \mathbf{y}_n \right) \rightarrow 0, \quad (4.14)$$

for any $M_n \rightarrow \infty$ as $n \rightarrow \infty$, and

$$\sup_{\beta_0 \in \ell_0[q_n]} \mathbb{E}_{\beta_0} \|\hat{\beta} - \beta_0\|_2^2 \lesssim q_n \log \left(\frac{n}{q_n} \right), \quad (4.15)$$

where $\hat{\beta}$ is the posterior mean under the NBP prior (4.13).

Proof. See Appendix B. □

Theorem 4.2 suggests that in the sparse normal means model, the hyperparameter b_n should be set comparable to the proportion of true signals q_n/n . This is consistent with the results in [3]. In the context of multiple hypothesis testing of normal means, Bai and Ghosh [3] found that in order for test procedures induced by the NBP prior (4.13) to asymptotically obtain the optimal Bayes risk under 0-1 loss, b_n should be the same order as q_n/n . Since the proportion of true signals is typically unknown, it should be estimated from the data. Some possible approaches are to compute the restricted marginal maximum likelihood (REML) estimator for b_n over the range $[1/n, 1]$, or to put a prior on the sparsity parameter b_n with support $[1/n, 1]$. These types of approaches are taken in [3, 38].

Theorem 4.2 also shows that theoretically optimal results for the normal means problem cannot be automatically generalized to the general linear regression setting. As we established in Theorem 4.1, in order to obtain near-minimax posterior contraction for the high-dimensional regression setup (4.1), we require a more conservative choice for the shape parameter b_n , where $b_n \lesssim p_n^{-(1+u)}$, for some $u > 0$. Meanwhile, in the sparse normal means problem, we require $b_n = (n/q_n)^{-\alpha} \succ n^{-\alpha}$, for some $\alpha \geq 1$, in order to achieve minimax posterior contraction. Since $p = n$ in the sparse normal means model (4.9), our results illustrate that the optimal choices for b_n in this setting are *not* necessarily optimal under (4.1).

5 Simulation Studies

For our simulation studies, we implement the NBP model (2.1) for model (1.1), with $c = d = 10^{-5}$ in the $\mathcal{IG}(c, d)$ prior on σ^2 , so that the prior is

fairly noninformative. For the beta prime prior $\beta'(a, b)$ in (2.1), we estimate a and b from Gibbs sampling with the Monte Carlo EM algorithm described in Section 3. To emphasize that we do not fix the hyperparameters (a, b) deterministically, we refer to the empirical Bayes variant of the NBP model (2.1) as the *self-adaptive* NBP model. Although fixing $a \in (1/2, \infty)$ and $b \lesssim p^{-(1+u)}$, for some $u > 0$, would lead to near-minimax posterior contraction under assumptions of sparsity, we prefer to learn the actual sparsity level from the data in case the true model is dense. As we illustrate in this section, the MML approach performs well in very sparse situations.

We use the EM/Gibbs sampling algorithm described in Section 3 to approximate the NBP posterior because it has provable statistical guarantees [11] and because the other software packages we used to implement competing Bayes estimators only used Gibbs sampling. We initialize $(a^{(0)}, b^{(0)}) = (0.01, 0.01)$ and update the EM algorithm every 100 iterations of the Gibbs sampler. We use a combination of block updating and fast sampling from structured multivariate Gaussians [6] to speed up our algorithm (see Appendix A for more details). Gibbs sampling implementation of the self-adaptive NBP model is available in the R package, `NormalBetaPrime`. Appendix A.2 also describes how to implement the variational EM approach for the self-adaptive NBP model if variational inference is preferred.

5.1 Variable Selection

Since the NBP model is absolutely continuous, it assigns zero mass to exactly sparse vectors. Therefore, selection must be performed using some posthoc method. Instead of using the posterior credible sets for selection, we propose using the “decoupled shrinkage and selection” (DSS) method proposed by Hahn and Carvalho [21]. Letting $\hat{\beta}$ denote the posterior mean of β , the DSS method performs variable selection by solving the optimization problem,

$$\hat{\gamma} = \arg \min_{\gamma} n^{-1} \|\mathbf{X}\hat{\beta} - \mathbf{X}\gamma\| + \lambda \|\gamma\|_0, \quad (5.1)$$

and choosing the nonzero entries in $\hat{\gamma}$ as the active set. Since (5.1) is an NP-hard combinatorial problem, Hahn and Carvalho [21] propose using local linear approximation, i.e. solving the following surrogate optimization problem instead:

$$\hat{\gamma} = \arg \min_{\gamma} n^{-1} \|\mathbf{X}\hat{\beta} - \mathbf{X}\gamma\| + \lambda \sum_{i=1}^p \frac{|\gamma_i|}{|\hat{\beta}_i|}, \quad (5.2)$$

where $\hat{\beta}_i$'s are the components in the posterior mean $\hat{\beta}$, and λ is chosen through cross-validation. We select the nonzero entries in $\hat{\gamma}$ from (5.2) as

the active set of covariates. The DSS method can be implemented easily in R with either the `lars` or `glmnet` package and is one of the variable selection methods available for the NBP prior in the R package, `NormalBetaPrime`. In our experience, the DSS method for selection works well in practice.

We remark that if (5.2) is used for variable selection, it will not select more than n variables. If potentially more than n variables are desired in the $p \gg n$ case, then we can implement elastic net regularization [42] on γ in (5.2) instead. This would allow for the selection of more than n variables.

5.2 Adaptivity to Different Sparsity Levels

In the first simulation study, we show that the self-adaptive NBP model has excellent performance under different sparsity levels. Under model (1.1), we generate a design matrix \mathbf{X} where the n rows are independently drawn from $\mathcal{N}_p(\mathbf{0}, \mathbf{\Gamma})$, $\mathbf{\Gamma} = (\Gamma_{ij})_{p \times p}$ with $\Gamma_{ij} = 0.5^{|i-j|}$, and then centered. We fix $\sigma^2 = 2$ for all settings. We set $n = 50, p = 100$, with varying levels of sparsity:

- Experiment 1: 10 active predictors (sparse model)
- Experiment 2: 20 active predictors (somewhat sparse model)
- Experiment 3: 30 active predictors (somewhat dense model)
- Experiment 4: 50 active predictors (dense model)

In all these settings, the true nonzero predictors in β_0 under (1.1) are generated from $\mathcal{U}([-2, -0.5] \cup [0.5, 2])$.

We compare the performance of the self-adaptive NBP prior with that of the minimax concave penalty (MCP) method [41], the smoothly clipped absolute deviation (SCAD) method [14], the Bayesian lasso [24], and the horseshoe [10]. MCP and SCAD produce unbiased estimates of large coefficients, whereas the original lasso [36] overshrinks large signals. The tuning parameters for MCP and SCAD are chosen through cross-validation. For the Bayesian lasso, the global tuning parameter is estimated by a gamma density with empirical Bayes hyperparameters, thus affording the Bayesian Lasso some additional adaptivity over its frequentist counterpart. For the horseshoe prior, we endow the global tuning parameter with the $\mathcal{C}^+(0, 1)$ prior in order to adapt to the underlying sparsity. These methods are available in the R packages: `ncvreg`, `momomvn`, and `horseshoe`.

For the NBP, horseshoe (HS), and Bayesian lasso (B-LASSO) priors, we run the Gibbs samplers for 20,000 iterations, discarding the first 10,000 as burn-in. We use the posterior median estimator $\hat{\beta}$ as our point estimator. We use the DSS method (5.1) for variable selection under the NBP and horseshoe priors. For the Bayesian lasso, the R package `monomvn` performs

variable selection by first placing a uniform prior on the model size and learning the sparsity level through this prior.

For each of our methods, we compute the mean squared error (MSE), mean squared predictor error (MPE), false discovery rate (FDR), false negative rate (FNR), and overall misclassification probability (MP):

$$\begin{aligned} \text{MSE} &= \|\widehat{\beta} - \beta_0\|_2^2/p, \\ \text{MPE} &= \|\mathbf{X}\widehat{\beta} - \mathbf{X}\beta_0\|_2^2/n \\ \text{FDR} &= \text{FP} / (\text{TP} + \text{FP}), \\ \text{FNR} &= \text{FN} / (\text{TN} + \text{FN}), \\ \text{MP} &= (\text{FP} + \text{FN})/p, \end{aligned}$$

where FP, TP, FN, and TN denote the number of false positives, true positives, false negatives, and true negatives respectively.

Table 1 shows our results averaged across 100 replications for the NBP, HS, B-LASSO, MCP, and SCAD methods. We see that across all of the various sparsity settings, the NBP has the lowest MSE *and* the lowest MPE (in the second setting with 20 active covariates, it ties with the horseshoe for the lowest estimation error). In the two sparse experiments (Experiments 1 and 2), the NBP and the HS give lower misclassification rates than the other methods. In Experiment 4, i.e. the densest setting, the NBP has significantly lower MSE and MPE than the other methods, and a slightly lower MP.

Overall, the self-adaptive NBP model seems to perform consistently well in all the different sparsity or non-sparsity settings. The performance of HS, MCP, and SCAD seems to degrade as the true model becomes more dense, whereas B-LASSO performs the worst in the sparsest setting, but much better in dense settings. Table 1 shows that in dense settings, the B-LASSO performs even better than MCP or SCAD. This seems to be because the HS, MCP, and SCAD models all favor sparsity by their construction (the HS because of its singularity at zero, and the MCP and SCAD models because of the regularization penalty). Meanwhile, the B-LASSO undershrinks signals near zero and slightly overshrinks large signals [12, 18], thus making the B-LASSO naturally inclined to favor dense models. In contrast, the self-adaptive NBP model is the only method that adapts to *both* sparse and dense settings.

Table 1: Simulation results for NBP, compared with the horseshoe (HS), Bayesian lasso (B-LASSO), MCP, and SCAD models, averaged across 100 replications when $n = 50, p = 100$.

Experiment 1: sparse model (10 active predictors)					
Method	MSE	MPE	FDR	FNR	MP
NBP	0.018	0.753	0.357	0.012	0.060
HS	0.020	0.993	0.200	0.022	0.040
B-LASSO	0.111	2.54	0.810	0.029	0.377
MCP	0.069	1.43	0.322	0.028	0.071
SCAD	0.049	1.30	0.421	0.018	0.084
Experiment 2: fairly sparse model (20 active predictors)					
Method	MSE	MPE	FDR	FNR	MP
NBP	0.081	2.10	0.200	0.041	0.069
HS	0.081	2.18	0.250	0.045	0.078
B-LASSO	0.225	3.99	0.748	0.070	0.373
MCP	0.493	6.52	0.416	0.133	0.186
SCAD	0.471	6.72	0.453	0.124	0.192
Experiment 3: somewhat dense model (30 active predictors)					
Method	MSE	MPE	FDR	FNR	MP
NBP	0.600	7.19	0.552	0.239	0.330
HS	0.676	17.54	0.593	0.260	0.350
B-LASSO	0.818	10.66	0.611	0.226	0.402
MCP	1.00	18.81	0.361	0.249	0.271
SCAD	0.905	21.93	0.390	0.241	0.269
Experiment 4: dense model (50 active predictors)					
Method	MSE	MPE	FDR	FNR	MP
NBP	0.762	9.64	0.172	0.317	0.310
HS	1.20	14.13	0.227	0.423	0.380
B-LASSO	1.27	16.62	0.396	0.404	0.400
MCP	2.07	48.95	0.299	0.469	0.449
SCAD	1.78	58.98	0.292	0.459	0.432

5.3 More Numerical Experiments with Large p

In this section, we consider two more settings with large p . In these experiments, the design matrix \mathbf{X} is generated the same way that it was in Section 5.2. The active predictors are randomly selected and fixed at a certain level, and the remaining covariates are set equal to zero.

- Experiment 5: ultra-sparse model with a few large signals ($n = 100, p = 500$, 8 active predictors set equal to 5)
- Experiment 6: dense model with many small signals ($n = 200, p = 400$, 200 active predictors set equal to 0.6)

In Experiment 5, we would expect the horseshoe prior to perform very well, since it contains a pole at zero and Cauchy-like tails. As a result of its concentration properties, the horseshoe squelches noise to zero more effectively than many other estimators, while leaving large signals mostly unshrunk [10, 12, 18, 25]. In a situation like Experiment 6, however, the horseshoe may have difficulty recovering the signals [39]. Meanwhile, the Bayesian lasso can still perform reasonably well in the setting of Experiment 6, because the B-LASSO does not shrink small entries near zero as heavily and because there are no large signals that would otherwise be overshrunk by the B-LASSO.

The self-adaptive NBP model manages to perform well in both these scenarios. We implement Experiments 5 and 6 for the NBP, HS, B-LASSO, MCP, and SCAD models. Table 2 shows our results averaged across 100 replications. We see that the NBP performs similarly as the HS in Experiment 5 and that both methods significantly outperform their competitors. The HS does perform the best in this ultra-sparse setting, but the NBP's performance seems quite comparable to the HS. Both the HS and the NBP give 0 for FDR, FNR, and MP, thus showing that both methods are able to adapt to ultra-sparse situations.

Table 2 also shows that in Experiment 6, the NBP model outperforms all the competing methods. The B-LASSO performs reasonably well in this setting with many small signals. The B-LASSO even has a lower MPE than the HS, but it still cannot beat the NBP in terms of prediction or estimation performance. Our results for Experiment 6 confirm that the self-adaptive NBP model is well-suited for estimation and variable selection in dense situations. In short, the marginal maximum likelihood method for selecting hyperparameters (a, b) in (2.1) gives the NBP prior the ability to adapt well to drastically different sparsity settings.

Table 2: Simulation results for NBP, compared with the horseshoe (HS), Bayesian Lasso (B-LASSO), MCP, and SCAD models, averaged across 100 replications.

Experiment 5: $n = 100, p = 500$, 8 active predictors set equal to 5.

Method	MSE	MPE	FDR	FNR	MP
NBP	0.0007	0.351	0	0	0
HS	0.0005	0.203	0	0	0
B-LASSO	0.018	2.272	0.919	0	0.181
MCP	0.088	0.637	0.139	0.001	0.013
SCAD	0.065	0.507	0.129	0.001	0.011

Experiment 6: $n = 200, p = 400$, 200 active predictors set equal to 0.6.

Method	MSE	MPE	FDR	FNR	MP
NBP	0.099	4.82	0.242	0.381	0.338
HS	0.150	12.68	0.247	0.410	0.368
B-LASSO	0.160	5.39	0.432	0.436	0.433
MCP	0.258	49.98	0.232	0.477	0.459
SCAD	0.200	45.63	0.241	0.454	0.423

There has been some recent work on refining the global parameters in the horseshoe and Bayesian lasso models, so that they can adapt better to underlying model characteristics (see, e.g., [38, 26, 40]). This certainly warrants investigation. However, it seems as though there are some inherent difficulties. The Bayesian lasso has exponentially decaying tails, so large signals are bound to be shrunk more aggressively under the B-LASSO than under polynomial-tailed priors like the horseshoe or the NBP priors. Meanwhile, the horseshoe always contains a singularity at zero, so it seems as though signals that are close to zero will tend to be shrunk more heavily.

On the other hand, we have shown that the self-adaptive NBP prior can overcome these difficulties and flexibly adapt to many different settings. If the true model is very sparse, the sparsity parameter b will be estimated to be very small and hence place heavier mass around zero. But if the true model is dense, the sparsity parameter b will be large, so the singularity at zero disappears and the prior becomes more diffuse. As a result, small signals are more easily detected by the self-adaptive NBP prior.

Table 3: Results for analysis of the Bardet-Biedl syndrome (BBS) dataset. The MSPE has been scaled by a factor of 100. In particular, all four models selected the three TFs, ACE2, SWI5, and SWI6 as significant.

Method	Number of Genes Selected	MSPE
NBP	32	0.387
HS	7	0.777
B-LASSO	101	0.604
MCP	6	0.567
SCAD	14	0.551

6 Analysis of a Gene Expression Data Set

We analyze a real data set from a study on Bardet-Biedl syndrome (BBS). This data set was first studied by Scheetz et al. [32] and is available in the R package `flare`. BBS is an autosomal recessive disorder that leads to progressive vision loss, extra fingers or toes, and kidney abnormalities. There is evidence that BBS is caused by mutation in the TRIM32 gene, a gene which itself may be influenced by other genes. This data set contains $n = 120$ samples with TRIM32 as the response variable and the expression levels of $p = 200$ other genes as the covariates.

To determine TRIM32’s association with these other genes, we implement the (self-adaptive) NBP, HS, B-LASSO, MCP, and SCAD models on this data set after centering and scaling \mathbf{X} and \mathbf{y} . To assess these methods’ predictive performance, we perform five-fold cross validation, using 80 percent of the data as our training set to obtain an estimate of β , $\hat{\beta}_{\text{train}}$. We take the posterior median as $\hat{\beta}_{\text{train}}$ and use it to compute the mean squared error of the residuals on the remaining 20 percent of the left-out data. We repeat this five times, using different training and test sets each time, and take the average MSE as our mean squared prediction error (MSPE).

To perform variable selection, we use the DSS method (5.1) described in Section 5.1. We also tried using 95 percent credible intervals for selection, but found that this approach seemed a bit too conservative. For example, if we used credible intervals for selection, the NBP and HS models both selected *zero* genes as being associated with TRIM32. This seems rather unrealistic, so we opted instead to use DSS for selection instead.

Table 3 shows the results of our analysis. The self-adaptive NBP model has the best predictive performance, with 32 genes selected as significantly associated with TRIM32. The B-LASSO selects a very dense model, but

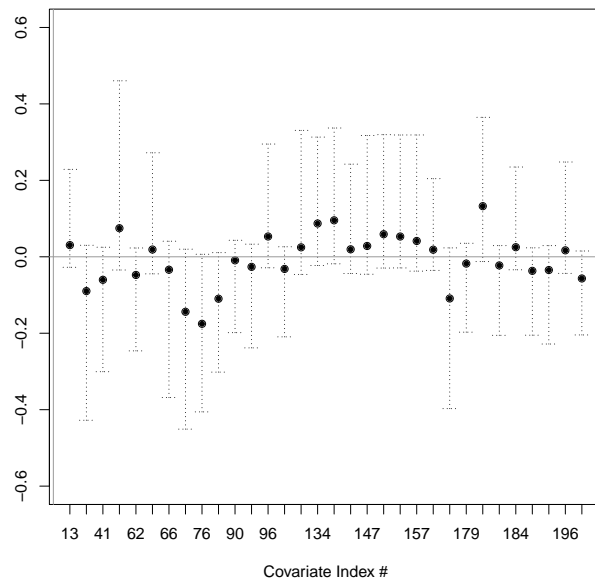


Figure 4: Posterior median and 95% credible intervals for the 32 genes that were selected as significantly associated with TRIM32 by the NBP model.

its performance lags behind NBP and SCAD. The HS and MCP methods resulted in more parsimonious models, with only 7 and 6 genes selected respectively, but their average prediction errors were both higher than NBP's. Our results suggest that there are a moderate number of signals in our data, but that the true underlying model is not quite as dense as the B-LASSO predicts.

Figure 4 plots the posterior 95 percent credible intervals for the 32 genes that the NBP model selected as significant. From this plot, we can assess the uncertainty quantification of our estimates. Figure 4 shows that the self-adaptive NBP prior is able to detect small gene expression values that are very close to zero. On this particular data set, the slightly more dense model determined by the NBP prior had much better prediction performance than the most parsimonious models (HS and MCP), suggesting that there may be a number of small signals in our data.

7 Concluding Remarks

In this paper, we have introduced the normal-beta prime (NBP) model for Bayesian linear regression. In order to make our prior self-adaptive, we in-

troduced an empirical Bayes approach to estimating the NBP’s hyperparameters through maximum marginal likelihood (MML). Our MML approach for estimating hyperparameters affords the NBP a great deal of flexibility and adaptivity to different levels of sparsity and different signal strengths. Moreover, the EM algorithm for estimating the hyperparameters avoids collapse to zero. The implementation of our model is available in the R package, `NormalBetaPrime`. We have also investigated the theoretical properties of our prior and shown that appropriate selection of hyperparameters enables it to achieve (near) minimax posterior contraction rates under the assumption of sparsity. Finally, we illustrated the (self-adaptive) NBP’s excellent finite sample performance through simulation studies and analysis of a gene expression data set. Our empirical studies show that the self-adaptive NBP’s automatic selection of hyperparameters from marginal maximum likelihood provides a viable alternative to cross-validation or hierarchical Bayes approaches for estimating unknown hyperparameters.

Our work lends strong support to the use of the general beta prime density as a scale parameter in Bayesian hierarchical models. Previously, Bai and Ghosh [3] proved that the NBP model has the Bayes Oracle property for multiple hypothesis testing. In this paper, we have shown that the NBP model can be used to build adaptive procedures in high-dimensional regression and that it achieves (near) minimax posterior contraction in high dimensions under sparsity assumptions.

Much still remains unknown. The NBP’s theoretical properties for uncertainty quantification and conditions under which the NBP achieves Bayes factor consistency or model selection consistency have yet to be investigated. Nevertheless, our results are encouraging. We conjecture that due to its flexibility, the NBP prior can also be extended to more complex models and other statistical procedures like density estimation or functional analysis, while retaining its strong empirical and theoretical properties.

A Technical Details of Posterior Approximation and Maximum Marginal Likelihood Estimation of (a, b)

In this section, we describe the the Gibbs sampling and mean field variational Bayes (MFVB) algorithms for approximating the posterior density under the NBP prior (2.1). In Section A.3, we also provide a proof of Theorem 3.1 that the M-step of the EM algorithm for obtaining the MML estimators of (a, b) always has a unique solution where $a^{(k)} > 0, b^{(k)} > 0$ at every k th

iteration, and therefore, our EM algorithm avoids collapse to zero.

A.1 Gibbs Sampling Implementation

Using the reparametrization (3.1), we see that NBP model admits the following full conditional densities. Let $\mathbf{D} = \text{diag}(\lambda_1^2 \xi_1^2, \dots, \lambda_p^2 \xi_p^2)$. The full conditional densities under the NBP model are:

$$\begin{aligned}
 \boldsymbol{\beta} | \text{rest} &\sim \mathcal{N}_p \left(\left(\mathbf{X}^\top \mathbf{X} + \mathbf{D}^{-1} \right)^{-1} \mathbf{X}^\top \mathbf{y}, \sigma^2 \left(\mathbf{X}^\top \mathbf{X} + \mathbf{D}^{-1} \right)^{-1} \right), \\
 \lambda_i^2 | \text{rest} &\stackrel{\text{ind}}{\sim} \mathcal{IG} \left(a + \frac{1}{2}, \frac{\beta_i^2}{2\sigma^2 \xi_i^2} + 1 \right), i = 1, \dots, p, \\
 \xi_i^2 | \text{rest} &\stackrel{\text{ind}}{\sim} \mathcal{GIG} \left(\frac{\beta_i^2}{\lambda_i}, 2, b - \frac{1}{2} \right), i = 1, \dots, p, \\
 \sigma^2 | \text{rest} &\sim \mathcal{IG} \left(\frac{n+p+2c}{2}, \frac{\|\mathbf{y} - \mathbf{X}\boldsymbol{\beta}\|_2^2 + \boldsymbol{\beta}^\top \mathbf{D}^{-1} \boldsymbol{\beta} + 2d}{2} \right),
 \end{aligned} \tag{A.1}$$

where $\mathcal{GIG}(a, b, p)$ denotes a generalized inverse Gaussian density with the pdf, $f(x; a, b, p) \propto x^{(p-1)} e^{-(a/x+bx)/2}$. From (A.1), Gibbs sampling is straightforward. Moreover, to save on computational time, the λ_i 's and ξ_i 's can be block-updated, and we can use the algorithm in [6] to sample from the full conditional for $\boldsymbol{\beta}$ in $O(n^2p)$ time.

To incorporate the EM algorithm for estimating (a, b) from Section 3 into our Gibbs sampler, we update (a, b) every $M = 100$ iterations of the Gibbs sampler by solving (3.4) and estimating the summand terms in (3.4) from the past M iterations of the Gibbs sampler. To assess convergence, we compute the ℓ_2 distance between $(\hat{a}^{(k-1)}, \hat{b}^{(k-1)})$ and $(\hat{a}^{(k)}, \hat{b}^{(k)})$ at the k th iteration of the EM Monte Carlo algorithm, and if it falls below a small tolerance $\delta > 0$, then we set our MML estimates as $(\hat{a}, \hat{b}) = (\hat{a}^{(k)}, \hat{b}^{(k)})$ and draw a final sample from the Gibbs sampler. We recommend setting $\delta = 10^{-6}$. If the ℓ_2 distance has not fallen below δ after a large number of iterations (we use $k = 100$, so that 10,000 total iterations of the Gibbs sampler have been sampled at this point), then we terminate the EM algorithm and use the final estimate from the 100th iteration as (\hat{a}, \hat{b}) . In our experience, even if the ℓ_2 distance between $(\hat{a}^{(k-1)}, \hat{b}^{(k-1)})$ and $(\hat{a}^{(k)}, \hat{b}^{(k)})$ does not quite fall underneath the small $\delta > 0$ after $k = 100$ iterations, the successive iterates are still very close to one another at this point. Thus, all these later estimates of (a, b) would have a similar effect on posterior inference.

A.2 Mean Field Variational Bayes Implementation

In a similar vein, we can implement the NBP model using mean field variational Bayes. Let $\boldsymbol{\lambda} = (\lambda_1^2, \dots, \lambda_p^2)$ and $\boldsymbol{\xi} = (\xi_1^2, \dots, \xi_p^2)$. We use the following approximation of the posterior:

$$q(\boldsymbol{\beta}, \boldsymbol{\lambda}, \boldsymbol{\xi}, \sigma^2 | \mathbf{y}) \approx q_1^*(\boldsymbol{\beta}) q_2^*(\boldsymbol{\lambda}), q_3^*(\boldsymbol{\xi}) q_4^*(\sigma^2), \quad (\text{A.2})$$

where

$$\begin{aligned} q_1^*(\boldsymbol{\beta}) &\sim \mathcal{N}_p(\boldsymbol{\beta}^*, \boldsymbol{\Sigma}^*), \\ q_2^*(\boldsymbol{\lambda}) &\stackrel{d}{=} \prod_{i=1}^p \mathcal{IG}(a^*, b_i^*), \\ q_3^*(\boldsymbol{\xi}) &\stackrel{d}{=} \prod_{i=1}^p \mathcal{GIG}(k_i^*, l^*, m^*), \\ q_4^*(\sigma^2) &\sim \mathcal{IG}(c^*, d^*), \end{aligned} \quad (\text{A.3})$$

and

$$\begin{aligned} \boldsymbol{\beta}^* &= (\mathbf{X}^\top \mathbf{X} + \mathbf{D}^*)^{-1} \mathbf{X}^\top \mathbf{y}, \quad \boldsymbol{\Sigma}^* = \mathbb{E}_{q_4^*}(\sigma^2) (\mathbf{X}^\top \mathbf{X} + \mathbf{D}^*)^{-1}, \\ \mathbf{D}^* &= \text{diag}(\mathbb{E}_{q_2^*}(\lambda_1^{-1}) \mathbb{E}_{q_3^*}(\xi_1^{-1}), \dots, \mathbb{E}_{q_2^*}(\lambda_p^{-1}) \mathbb{E}_{q_3^*}(\xi_p^{-1})), \quad a^* = a + \frac{1}{2}, \\ b_i^* &= \frac{1}{2} \mathbb{E}_{q_1^*}(\beta_i^2) \mathbb{E}_{q_4^*}(\sigma^{-2}) \mathbb{E}_{q_3^*}(\xi_i^{-1}) + 1, \quad k_i = \mathbb{E}_{q_1^*}(\beta_i^2) \mathbb{E}_{q_2^*}(\lambda_i^{-1}), \quad i = 1, \dots, p, \\ l^* &= 2, \quad m^* = b - \frac{1}{2}, \quad c^* = \frac{n+p+2c}{2}, \\ d^* &= \frac{\mathbb{E}_{q_1^*}(\|\mathbf{y} - \mathbf{X}\boldsymbol{\beta}\|_2^2) + \mathbb{E}_{q_1^*}(\boldsymbol{\beta}^\top) \mathbf{D}^* \mathbb{E}_{q_1^*}(\boldsymbol{\beta}) + 2d}{2}, \end{aligned} \quad (\text{A.4})$$

From (A.4), we can construct the MFVB coordinate ascent updates easily, and posterior inference on $\boldsymbol{\beta}$ can be carried out through $q_1^*(\boldsymbol{\beta})$. In (A.4), we can compute the expectations with respect to q_2^* , q_3^* , and q_4^* in closed form, using standard properties of the \mathcal{IG} and \mathcal{GIG} densities. Using stochastic variational inference, at the t th iteration, we replace $\mathbb{E}_{q_1^{*(t)}}[f(\boldsymbol{\beta})]$ in (A.4) with simply $f(\boldsymbol{\beta}^{(t)})$ for any function f of $\boldsymbol{\beta}$. At each iteration, we compute the evidence lower bound (ELBO),

$$\mathcal{L} = \mathbb{E}_q \log f(\mathbf{y}, \boldsymbol{\beta}, \boldsymbol{\lambda}, \boldsymbol{\xi}, \sigma^2) - \mathbb{E}_q \log q(\boldsymbol{\beta}, \boldsymbol{\lambda}, \boldsymbol{\xi}, \sigma^2), \quad (\text{A.5})$$

where f is the joint density over \mathbf{y} and all parameters, the expectations in (A.5) are taken with respect to the density q in (A.2). Convergence is assessed by computing the absolute difference, $\text{dif} = |\mathcal{L}^{(t)} - \mathcal{L}^{(t-1)}|$, at each iteration, and terminating the algorithm if $\text{dif} < \delta$, for some small tolerance $\delta > 0$. We run the MFVB algorithm until convergence or until a maximum of 1000 iterations have been reached.

To incorporate the EM algorithm for computing hyperparameters (a, b) into the MFVB scheme, we solve for (a, b) in (3.4) in every iteration of coordinate ascent algorithm, using $\mathbb{E}_{q_2^{*(t-1)}, a^{(t-1)}} [\ln(\lambda_i^2)]$ and $\mathbb{E}_{q_3^{*(t-1)}, b^{(t-1)}} [\ln(\xi_i^2)]$ in place of the summands in (3.4) at the t th iteration. Namely, these expectations are given by:

$$\begin{aligned}\mathbb{E}_{q_2^{*(t-1)}, a^{(t-1)}} [\ln(\lambda_i^2)] &= \ln \left(b_i^{*(t-1)} \right) - \psi \left(a^{*(t-1)} \right), \\ \mathbb{E}_{q_3^{*(t-1)}, b^{(t-1)}} [\ln(\xi_i^2)] &= \ln \left(\frac{\sqrt{k_i^{*(t-1)}}}{\sqrt{l^*}} \right) + \frac{\partial}{\partial m^{*(t-1)}} \ln \left[K_{m^{*(t-1)}} \left(\sqrt{k_i^{*(t-1)}} l^* \right) \right],\end{aligned}\tag{A.6}$$

where $K_p(\cdot)$ denotes the modified Bessel function of the second kind, and $a^{*(t-1)}$, $b_i^{*(t-1)}$, $k_i^{*(t-1)}$, l^* , and $m^{*(t-1)}$ are taken from the $(t-1)$ st iteration and defined in (A.4). The derivative in the second equation in (A.6) can be computed using numerical differentiation.

A.3 Proof of Theorem 3.1

Proof of Theorem 3.1. At the k th iteration of the EM algorithm, the (a, b) that solves (3.4) is

$$\begin{aligned}\psi(a) &= -\frac{1}{p} \sum_{i=1}^p U_i(\lambda_i^2), \quad a > 0, \\ \psi(b) &= \frac{1}{p} \sum_{i=1}^p V_i(\xi_i^2), \quad b > 0,\end{aligned}\tag{A.7}$$

where $U_i(\lambda_i^2)$ is an estimate of $\mathbb{E}_{a^{(k-1)}} [\ln(\lambda_i^2) | \mathbf{y}]$ and $V_i(\xi_i^2)$ is an estimate of $\mathbb{E}_{b^{(k-1)}} [\ln(\xi_i^2) | \mathbf{y}]$ taken from either the Gibbs sampler or the MFVB coordinate ascent algorithm. Since the λ_i 's and ξ_i 's, $i = 1, \dots, p$, are strictly greater than zero and are drawn from \mathcal{IG} and \mathcal{GIG} densities in the Gibbs sampling or the MFVB algorithms (and thus, expectations of $\ln(\lambda_i^2)$ and $\ln(\xi_i^2)$, $i = 1, \dots, p$, are well-defined and finite), U_i and V_i , $i = 1, \dots, p$, exist and are finite.

The digamma function $\psi(x)$ is continuous and monotonically increasing for all $x \in (0, \infty)$, with a range of $(-\infty, \infty)$ on the domain of positive reals. Therefore, for any $y \in \mathbb{R}$, there exists a unique $x \in (0, \infty)$ so that $\psi(x) = y$. Since we impose the constraint that $a > 0$, there must be a unique $\hat{a}^{(k)} > 0$ that solves the first equation in (A.7). Similarly, there exists a unique $\hat{b}^{(k)} > 0$ that solves the second equation in (A.7). \square

B Proofs for Section 4

In this section, we provide proofs of Theorems 4.1 and 4.2 and Proposition 4.1.

B.1 Proof of Theorem 4.1 (High-Dimensional Regression)

Before proving Theorem 4.1, we restate the main results on posterior consistency from Song and Liang [34]. Proposition B.1 is a restatement of Theorems A.1 and A.2 in [34].

Proposition B.1. *Consider the linear regression model (4.1) and suppose that condition (A1)-(A5) hold. Suppose that the prior for $\pi(\boldsymbol{\beta}, \sigma^2)$ is of the form (4.3). Suppose $r_n = M\sqrt{s \log p_n/n}$, where $M > 0$ is sufficiently large. If the density $g(\cdot)$ in (4.3) satisfies*

$$\begin{aligned} 1 - \int_{-k_n}^{k_n} g(x) dx &\leq p_n^{-(1+u)}, \\ -\log \left(\inf_{x \in [-E_n, E_n]} g(x) \right) &= O(\log p_n), \end{aligned} \tag{B.1}$$

where $u > 0$ is a constant and $k_n \asymp \sqrt{s \log p_n/n}/p_n$, then the following results hold:

$$\begin{aligned} \Pr_{\beta_0} \left(\Pi(\boldsymbol{\beta} : \|\boldsymbol{\beta} - \boldsymbol{\beta}_0\|_2 \geq c_1 \sigma r_n | \mathbf{y}_n) \geq e^{-c_2 n r_n^2} \right) &\leq e^{-c_3 n r_n^2}, \\ \Pr_{\beta_0} \left(\Pi(\boldsymbol{\beta} : \|\boldsymbol{\beta} - \boldsymbol{\beta}_0\|_1 \geq c_1 \sigma \sqrt{s} r_n | \mathbf{y}_n) \geq e^{-c_2 n r_n^2} \right) &\leq e^{-c_3 n r_n^2}, \\ \Pr_{\beta_0} \left(\Pi(\boldsymbol{\beta} : \|\mathbf{X}_n \boldsymbol{\beta} - \mathbf{X}_n \boldsymbol{\beta}_0\|_2 \geq c_0 \sigma \sqrt{n} r_n | \mathbf{y}_n) < 1 - e^{-c_2 n r_n^2} \right) &\leq e^{-c_3 n r_n^2}, \\ \Pr_{\beta_0} \left(\Pi(\boldsymbol{\beta} : \text{at least } \tilde{p} \text{ entries of } |\boldsymbol{\beta}/\sigma| \text{ are larger than } k_n | \mathbf{y}_n) > e^{-c_2 n r_n^2} \right) &\leq e^{-c_3 n r_n^2}, \end{aligned}$$

for some constants $c_0, c_1, c_2, c_3 > 0$, and $\tilde{p} \asymp s$.

Before proving Theorem 4.1, we first prove a lemma.

Lemma B.1. *Suppose that $a \in (1/2, \infty)$ and $b_n \rightarrow 0$ as $n \rightarrow \infty$. Then*

$$\frac{\Gamma(a + b_n)}{\Gamma(a)\Gamma(b_n)} \asymp b_n. \tag{B.2}$$

Proof of Lemma B.1. Rewrite (B.2) as

$$\frac{\Gamma(a + b_n)}{\Gamma(a)\Gamma(b_n)} = \frac{b_n \Gamma(a + b_n)}{\Gamma(a)\Gamma(b_n + 1)}. \tag{B.3}$$

Since $a \in (1/2, \infty)$, we have $\Gamma(a) < \Gamma(6a)$. To see this, note that $\Gamma(1/2) = \sqrt{\pi}$ and $\Gamma(3) = 2$, and that the function $\Gamma(x)$ is monotonic decreasing on $[1/2, x_{\min}]$ and monotonic increasing on (x_{\min}, ∞) , where x_{\min} is the local minimum of the gamma function on the positive reals ($x_{\min} \approx 1.46163$). Let $c^* = \Gamma(x_{\min}) \approx 0.885603$. Since $b_n = o(1)$, we have

$$\frac{\Gamma(a + b_n)}{\Gamma(a)\Gamma(b_n + 1)} \lesssim \frac{\Gamma(6a)}{\Gamma(a)c^*}, \quad (\text{B.4})$$

and

$$\frac{\Gamma(a + b_n)}{\Gamma(a)\Gamma(b_n + 1)} \gtrsim \frac{c^*}{\Gamma(a)\Gamma(1)}, \quad (\text{B.5})$$

and so combining (B.3)-(B.5), it is clear that (B.2) holds. \square

Proof of Theorem 4.1. By Proposition B.1, it is sufficient to verify that the NBP prior for each coefficient $\pi(\beta_i), i = 1, \dots, p_n$, satisfies the two conditions (B.1). We first verify the first condition. Let $g(\cdot)$ be the marginal pdf of $\pi(\beta)$ for a single coefficient β . The pdf $g(x)$ under the NBP prior is

$$g(x) = \frac{\Gamma(a + b_n)}{(2\pi)^{1/2}\Gamma(a)\Gamma(b)} \int_0^\infty \exp\left(-\frac{x^2}{2\omega^2}\right) (\omega^2)^{a-3/2} (1 + \omega^2)^{-a-b_n} d\omega^2. \quad (\text{B.6})$$

By the symmetry of $g(x)$ and Fubini's Theorem, we have from (B.6) that

$$\begin{aligned} 1 - \int_{-k_n}^{k_n} g(x) dx &= 2 \int_{k_n}^\infty g(x) dx \\ &= \frac{2\Gamma(a + b_n)}{(2\pi)^{1/2}\Gamma(a)\Gamma(b)} \int_{k_n}^\infty \int_0^\infty \exp\left(-\frac{x^2}{2\omega^2}\right) (\omega^2)^{a-3/2} (1 + \omega^2)^{-a-b_n} d\omega^2 dx \\ &= \frac{\Gamma(a + b_n)}{\Gamma(a)\Gamma(b_n)} \int_0^\infty (\omega^2)^{a-1} (1 + \omega^2)^{-a-b_n} \left[2 \int_{k_n}^\infty (2\pi\omega^2)^{-1/2} \exp\left(-\frac{x^2}{2\omega^2}\right) dx \right] d\omega^2 \end{aligned} \quad (\text{B.7})$$

Letting $X \sim \mathcal{N}(0, \omega^2)$, we see the inner integral in (B.7) is $\Pr(|X| \geq k_n)$. We use the concentration inequality, $\Pr(|X| \geq k_n) \leq 2e^{-k_n^2/2\omega^2}$, to further bound (B.7) above as

$$\begin{aligned} &2 \int_{k_n}^\infty g(x) dx \\ &\leq \frac{2\Gamma(a + b_n)}{\Gamma(a)\Gamma(b_n)} \int_0^\infty (\omega^2)^{a-1} (1 + \omega^2)^{-a-b_n} e^{-k_n^2/2\omega^2} d\omega^2 := I_{a, b_n} \quad (\text{say}). \end{aligned} \quad (\text{B.8})$$

We now consider two cases separately: $1/2 < a < 1$ and $a \geq 1$.

- **Case 1:** Suppose that $1/2 < a < 1$. For any $a \in (0, 1)$ and $b > 0$, the beta prime distribution $\beta'(a, b)$ is stochastically dominated by $\beta'(1, b)$ (by the monotone likelihood ratio property of the beta family). Additionally, $\exp(-k_n^2/(2\omega^2))$ is increasing in ω^2 with 1 as the upper bound. Thus, we have from (B.8) that

$$\begin{aligned}
I_{a,b_n} &\leq I_{1,b_n} = 2b_n \int_0^\infty (1 + \omega^2)^{-1-b_n} e^{-k_n^2/2\omega^2} d\omega^2 \\
&\leq 2b_n \int_0^\infty (1 + \omega^2)^{-1} d\omega^2 \\
&= \pi b_n \\
&\lesssim p_n^{-(1+u)}
\end{aligned} \tag{B.9}$$

where in the final inequality, we used our assumption that $b_n \lesssim p_n^{-(1+u)}$, for some $u > 0$.

- **Case 2:** Suppose that $a \geq 1$. Using Lemma B.1, we have

$$\begin{aligned}
I_{a,b_n} &\lesssim b_n \int_0^\infty (\omega^2)^{a-1} (1 + \omega^2)^{-a-b_n} e^{-k_n^2/2\omega^2} d\omega^2 \\
&= b_n \int_0^\infty \left(\frac{\omega^2}{1 + \omega^2} \right)^{a-1} (1 + \omega^2)^{-1-b_n} e^{-k_n^2/2\omega^2} d\omega^2 \\
&\leq b_n \int_0^\infty (1 + \omega^2)^{-1} d\omega^2 \\
&= b_n \left(\frac{\pi}{2} \right) \\
&\lesssim p_n^{-(1+u)},
\end{aligned} \tag{B.10}$$

where we again use the assumption about the rate of decay of b_n .

Combining (B.8)-(B.10), we have that for any $a \in (1/2, \infty)$ and $b_n \lesssim p_n^{-(1+u)}$, $u > 0$, the first condition of (B.1) holds.

We now show that the second condition of (B.1) also holds under our assumptions on (a, b_n) and our assumption on the rate of growth on E_n in Assumption (A5). With a change of variables, $z = x^2/2\omega^2$, in (B.6), we can rewrite the marginal pdf of the NBP prior, $g(x)$, as

$$g(x) = \frac{\Gamma(a + b_n)}{2^{1-b_n} \pi^{1/2} \Gamma(a) \Gamma(b_n)} (x^2)^{a-1/2} \int_0^\infty e^{-z} z^{b_n-1/2} (x^2 + 2z)^{-a-b_n} dz. \tag{B.11}$$

By the symmetry of $g(x)$, the infimum of $g(x)$ on the interval $[-E_n, E_n]$ obviously occurs at either $-E_n$ or E_n . From (B.2), (B.11), and the assumptions that E_n is nondecreasing, $a \in (1/2, \infty)$, and $b_n = o(1)$, we have

$$\begin{aligned}
\inf_{x \in [-E_n, E_n]} g(x) &\gtrsim b_n (E_n^2)^{a-1/2} \int_0^\infty e^{-z} z^{b_n-1/2} (E_n^2 + 2z)^{-a-b_n} dz \\
&\gtrsim b_n \int_{1/2}^1 e^{-z} z^{b_n-1/2} (E_n^2 + 2z)^{-a-b_n} dz \\
&\gtrsim b_n (E_n^2 + 2)^{-a-b_n} \\
&\asymp b_n E_n^{-2a}.
\end{aligned} \tag{B.12}$$

By assumption, $b_n \lesssim p_n^{-(1+u)}$, $u > 0$, and $\log(E_n) = O(\log p_n)$. Therefore, it follows from (B.12) that

$$\begin{aligned}
-\log \left(\inf_{x \in [-E_n, E_n]} g(x) \right) &\lesssim -\log(p_n^{-(1+u)}) + 2a \log(p_n) \\
&\lesssim \log p_n,
\end{aligned} \tag{B.13}$$

i.e. the second condition in (B.1) holds.

We have shown that as long as $a \in (1/2, \infty)$, $b_n \lesssim p_n^{-(1+u)}$ for some $u > 0$, and $\log(E_n) = O(\log p_n)$ in Assumption (A5), the two conditions (B.1) in Proposition B.1 are satisfied. Hence, Theorem 4.1 has been proven. \square

B.2 Proofs for the Sparse Normal Means Model

B.2.1 Proof of Proposition 4.1

We first prove Proposition 4.1 which shows that the NBP_n prior (4.13) does not satisfy condition (4.12). Consequently, our prior does not seem to satisfy the sufficient conditions of [37] for minimax posterior contraction.

Proof of Proposition 4.1. For convenience, we restate the beta prior density with shape parameters (a, b_n) below.

$$\pi_n(u) = \frac{\Gamma(a + b_n)}{\Gamma(a)\Gamma(b_n)} u^{a-1} (1 + u)^{-a-b_n} \tag{B.14}$$

Using Lemma B.1, we have from (B.14) that

$$\int_0^1 \pi_n(u) du \lesssim b_n \int_0^1 u^{a-1} (1 + u)^{-a-b_n} du$$

$$\begin{aligned}
&\leq b_n \int_0^1 u^{a-1} du \\
&= a^{-1} b_n = O(b_n).
\end{aligned}$$

Thus, under our conditions on a and b_n , we have shown that the integral of the beta prime density (B.14) on the interval $[0, 1]$ is always of the order, $O(b_n)$. \square

B.2.2 Proof of Theorem 4.2

We now prove Theorem 4.2, which shows that the NBP $_n$ prior (4.13) *does* indeed obtain the minimax posterior contraction rate, despite not satisfying one of the conditions for minimax posterior contraction from [37]. Our proof techniques follow closely those of van der Pas et al. [39] and Ghosh and Chakrabarti [17].

We first prove seven lemmas which are instrumental for proving Theorem 4.2. For Lemmas B.2-B.8, we denote $T(y) = \{\mathbb{E}(1 - \kappa|y)\}y$ as the posterior mean under (4.13) for a single observation y , where $\kappa = 1/(1 + \omega^2)$.

Lemma B.2. *Let $\kappa = 1/(1 + \omega^2)$ for a single β in model (4.13). Fix $\eta \in (0, 1), \delta \in (0, 1)$. Then for any $a \in (1/2, \infty)$ and $b_n \in (0, 1)$,*

$$\mathbb{E}(1 - \kappa|y) \leq e^{y^2/2} \left(\frac{b_n}{a + b_n + 1/2} \right), \quad (\text{B.15})$$

and

$$\Pr(\kappa > \eta|y) \leq \frac{\left(a + \frac{1}{2}\right) (1 - \eta)^{b_n}}{b_n (\eta \delta)^{a + \frac{1}{2}}} \exp\left(-\frac{\eta(1 - \delta)}{2} y^2\right). \quad (\text{B.16})$$

Proof. See proofs of Theorems 2.1 and Theorem 2.3 in Bai and Ghosh [3]. \square

Lemma B.3. *Let $T(y)$ be the posterior mean under (4.13) for a single observation y drawn from $\mathcal{N}(\beta, 1)$. Suppose we have constants $\eta \in (0, 1)$, $\delta \in (0, 1)$, $a \in (\frac{1}{2}, \infty)$, and $b_n \in (0, 1)$, where $b_n \rightarrow 0$ as $n \rightarrow \infty$. Then for any $d > 2$ and fixed n , $|T(y) - y|$ can be bounded above by a real-valued function $h_n(x)$, depending on d and satisfying the following:*

For any $\rho > d$, $h_n(\cdot)$ satisfies

$$\lim_{n \rightarrow \infty} \sup_{|y| > \sqrt{\rho \log\left(\frac{1}{b_n}\right)}} h_n(y) = 0. \quad (\text{B.17})$$

Proof of Lemma B.3. It is straightforward to check that for $\kappa = 1/(1 + \omega)$,

$$\pi(\kappa|y) \propto \exp\left(-\frac{\kappa y^2}{2}\right) \kappa^{a-1/2} (1-\kappa)^{b_n-1}, \quad \kappa \in (0, 1). \quad (\text{B.18})$$

Fix $\eta \in (0, 1), \delta \in (0, 1)$. First observe that

$$\begin{aligned} |T(y) - y| &= |y\mathbb{E}(\kappa|y)| \\ &\leq |y\mathbb{E}(\kappa 1\{\kappa < \eta\})| + |y\mathbb{E}(\kappa 1\{\kappa > \eta\})|. \end{aligned} \quad (\text{B.19})$$

We consider the two terms in (B.19) separately. From (B.18) and the fact that $(1-\kappa)^{b_n-1}$ is increasing in $\kappa \in (0, 1)$ when $b_n \in (0, 1)$, we have

$$\begin{aligned} |y\mathbb{E}(\kappa 1\{\kappa < \eta\})| &= \left| y \frac{\int_0^\eta \kappa \cdot \kappa^{a-1/2} (1-\kappa)^{b_n-1} e^{-\kappa y^2/2} d\kappa}{\int_0^1 \kappa^{a-1/2} (1-\kappa)^{b_n-1} e^{-\kappa y^2/2} d\kappa} \right| \\ &\leq |y| \left| (1-\eta)^{b_n-1} \frac{\int_0^\eta \kappa^{a+1/2} e^{-\kappa y^2/2} d\kappa}{\int_0^1 \kappa^{a-1/2} e^{-\kappa y^2/2} d\kappa} \right| \\ &= (1-\eta)^{b_n-1} \left| \frac{\int_0^{\eta y^2} \left(\frac{t}{y^2}\right)^{a+1/2} e^{-t/2} dt}{\int_0^{y^2} \left(\frac{t}{y^2}\right)^{a-1/2} e^{-t/2} dt} \right| |y| \\ &= (1-\eta)^{b_n-1} \left| \frac{1}{y^2} \frac{\int_0^{\eta y^2} t^{a+1/2} e^{-t/2} dt}{\int_0^{y^2} t^{a-1/2} e^{-t/2} dt} \right| |y| \\ &\leq (1-\eta)^{b_n-1} \left| \frac{\int_0^\infty t^{a+1/2} e^{-t/2} dt}{\int_0^{y^2} t^{a-1/2} e^{-t/2} dt} \right| |y|^{-1} \\ &= C(n) \left[\left| \int_0^{y^2} t^{a-1/2} e^{-t/2} dt \right| \right]^{-1} |y|^{-1} \\ &= h_1(y) \quad (\text{say}), \end{aligned} \quad (\text{B.20})$$

where we use a change of variables $t = \kappa y^2$ in the second equality, and $C(n) = (1-\eta)^{b_n-1} \left(\frac{\Gamma(1)\Gamma(a+3/2)}{\Gamma(a+5/2)} \right) = (1-\eta)^{b_n-1} \left(a + \frac{3}{2} \right)^{-1}$. Next, we observe that since $\kappa \in (0, 1)$,

$$\begin{aligned} |y\mathbb{E}(\kappa 1\{\kappa > \eta\})| &\leq |y \Pr(\kappa > \eta|y)| \\ &\leq \frac{\left(a + \frac{1}{2}\right) (1-\eta)^{b_n}}{b_n(\eta\delta)^{a+1/2}} |y| \exp\left(-\frac{\eta(1-\delta)}{2} y^2\right) \\ &= h_2(y) \quad (\text{say}), \end{aligned} \quad (\text{B.21})$$

where we use (B.16) from Lemma B.2 for the second inequality.

Let $h_n(y) = h_1(y) + h_2(y)$. Combining (B.19)-(B.21), we have that for every $y \in \mathbb{R}$ and fixed n ,

$$|T(y) - y| \leq h_n(y), \quad (\text{B.22})$$

Observe from (B.20) that for fixed n , $h_1(y)$ is strictly decreasing in $|y|$. Therefore, we have that for any fixed n and $\rho > 0$,

$$\sup_{|y| > \sqrt{\rho \log\left(\frac{1}{b_n}\right)}} h_1(y) \leq C(n) \left[\left| \sqrt{\rho \log\left(\frac{1}{b_n}\right)} \int_0^{\rho \log\left(\frac{1}{b_n}\right)} t^{a-1/2} e^{-t/2} dt \right| \right]^{-1},$$

and since $b_n \rightarrow 0$ as $n \rightarrow \infty$, this implies that

$$\lim_{n \rightarrow \infty} \sup_{|y| > \sqrt{\rho \log\left(\frac{1}{b_n}\right)}} h_1(y) = 0. \quad (\text{B.23})$$

Next, observe that from (B.21) that for fixed n , $h_2(y)$ is eventually decreasing in $|y|$ with a maximum when $|y| = \frac{1}{\sqrt{\eta(1-\delta)}}$. Therefore, for sufficiently large n , we have

$$\sup_{|y| > \sqrt{\rho \log\left(\frac{1}{b_n}\right)}} h_2(y) \leq h_2\left(\sqrt{\rho \log\left(\frac{1}{b_n}\right)}\right).$$

Letting $K \equiv K(a, \eta, \delta) = \frac{(a+\frac{1}{2})}{(\eta\delta)^{a+1/2}}$, we have from (B.21) and the fact that $0 < b_n < 1$ for all n that

$$\begin{aligned} \lim_{n \rightarrow \infty} h_2\left(\sqrt{\rho \log\left(\frac{1}{b_n}\right)}\right) &= K \lim_{n \rightarrow \infty} \frac{(1-\eta)^{b_n}}{b_n} \sqrt{\rho \log\left(\frac{1}{b_n}\right)} e^{-\frac{\eta(1-\delta)}{2} \rho \log\left(\frac{1}{b_n}\right)} \\ &\leq K \lim_{n \rightarrow \infty} \frac{1}{b_n} \sqrt{\rho \log\left(\frac{1}{b_n}\right)} e^{\frac{\eta(1-\delta)}{2} \log(b_n^\rho)} \\ &= K \sqrt{\rho} \lim_{n \rightarrow \infty} (b_n)^{\frac{\eta(1-\delta)}{2} (\rho - \frac{2}{\eta(1-\delta)})} \sqrt{\log\left(\frac{1}{b_n}\right)} \\ &= \begin{cases} 0 & \text{if } \rho > \frac{2}{\eta(1-\delta)}, \\ \infty & \text{otherwise,} \end{cases} \end{aligned}$$

from which it follows that

$$\lim_{n \rightarrow \infty} \sup_{|y| > \sqrt{\rho \log(\frac{1}{b_n})}} h_2(y) = \begin{cases} 0 & \text{if } \rho > \frac{2}{\eta(1-\delta)}, \\ \infty & \text{otherwise.} \end{cases} \quad (\text{B.24})$$

Combining (B.23) and (B.24), we have for $h_n(y) = h_1(y) + h_2(y)$ that

$$\lim_{n \rightarrow \infty} \sup_{|y| > \sqrt{\rho \log(\frac{1}{b_n})}} h_n(y) = \begin{cases} 0 & \text{if } \rho > \frac{2}{\eta(1-\delta)}, \\ \infty & \text{otherwise.} \end{cases} \quad (\text{B.25})$$

Since $\eta \in (0, 1)$, $\delta \in (0, 1)$, it is clear that any real number larger than 2 can be expressed in the form $\frac{2}{\eta(1-\delta)}$. For example, taking $\eta = \frac{5}{6}$ and $\delta = \frac{1}{5}$, we obtain $\frac{2}{\eta(1-\delta)} = 3$. Hence, given any $d > 2$, choose $0 < \eta, \delta < 1$ such that $c = \frac{2}{\eta(1-\delta)}$. Clearly, $h_n(\cdot)$ depends on d . Following (B.22) and (B.25), we see that $|T(y) - y|$ is uniformly bounded above by $h_n(y)$ for all n and $d > 2$ and that condition (B.17) is also satisfied when $d > 2$. This completes the proof. \square

Lemma B.4. *Let $T(y)$ be the posterior mean and let $\text{Var}(\beta|y)$ be the posterior variance under (4.13). Then for a single observation $y \sim \mathcal{N}(\beta, 1)$, $\text{Var}(\beta|y)$ can be represented by the following identities:*

$$\text{Var}(\beta|y) = \frac{T(y)}{y} - (T(y) - y)^2 + y^2 \frac{\int_0^1 \kappa^{a+3/2} (1-\kappa)^{b_n-1} e^{-\kappa y^2/2} d\kappa}{\int_0^1 \kappa^{a-1/2} (1-\kappa)^{b_n-1} e^{-\kappa y^2/2} d\kappa}, \quad (\text{B.26})$$

and

$$\text{Var}(\beta|y) = \frac{T(y)}{y} - T(y)^2 + y^2 \frac{\int_0^1 \kappa^{a-1/2} (1-\kappa)^{b_n+1} e^{-\kappa y^2/2} d\kappa}{\int_0^1 \kappa^{a-1/2} (1-\kappa)^{b_n-1} e^{-\kappa y^2/2} d\kappa}, \quad (\text{B.27})$$

both of which satisfy the bound $\text{Var}(\beta|y) \leq 1 + y^2$.

Proof of Lemma B.4. We first prove (B.26). By the law of the iterated variance and the fact that $\beta|(\kappa, y) \sim N((1-\kappa)y, 1-\kappa)$, we have

$$\begin{aligned} \text{Var}(\beta|y) &= \mathbb{E}[\text{Var}(\beta|\kappa, y)] + \text{Var}[\mathbb{E}(\beta|\kappa, y)] \\ &= \mathbb{E}(1-\kappa|y) + \text{Var}[(1-\kappa)y|y] \\ &= \mathbb{E}(1-\kappa|y) + y^2 \text{Var}(\kappa|y) \\ &= \mathbb{E}[(1-\kappa|y) + y^2 \mathbb{E}(\kappa^2|y) - y^2 [\mathbb{E}(\kappa|y)]^2]. \end{aligned}$$

Since $y - T(y) = y\mathbb{E}(\kappa|y)$, we rewrite the above as

$$\text{Var}(\beta|y) = \frac{T(y)}{y} - (T(y) - y)^2 + y^2 \frac{\int_0^1 \kappa^{a+3/2} (1-\kappa)^{b_n-1} e^{-\kappa y^2/2} d\kappa}{\int_0^1 \kappa^{a-1/2} (1-\kappa)^{b_n-1} e^{-\kappa y^2/2} d\kappa}.$$

Since $\kappa^{a+\frac{3}{2}} \leq \kappa^{a+\frac{1}{2}}$ for all $a \in \mathbb{R}$ when $\kappa \in (0, 1)$, it follows that the above display can be bounded from above as $\text{Var}(\beta|y) \leq 1 + y^2$.

Next, we show that (B.27) holds. We may alternatively represent $\text{Var}(\beta|x)$ as

$$\begin{aligned} \text{Var}(\beta|y) &= \mathbb{E}(1 - \kappa|y) + y^2 \mathbb{E}[(1 - \kappa)^2|y] - y^2 \mathbb{E}^2[(1 - \kappa)|y] \\ &= \frac{T(y)}{y} - T(y)^2 + y^2 \frac{\int_0^1 \kappa^{a-1/2} (1-\kappa)^{b_n+1} e^{-\kappa y^2/2} d\kappa}{\int_0^1 \kappa^{a-1/2} (1-\kappa)^{b_n-1} e^{-\kappa y^2/2} d\kappa}. \end{aligned}$$

Since $(1 - \kappa)^{b_n+1} \leq (1 - \kappa)^{b_n-1}$ for all $b_n \in \mathbb{R}$ when $\kappa \in (0, 1)$, it follows that the above display can also be bounded from above as $\text{Var}(\beta|y) \leq 1 + y^2$. \square

Lemma B.5. *Let $\text{Var}(\beta|y)$ be the posterior variance under (4.13) for a single observation y drawn from $\mathcal{N}(\beta, 1)$. Suppose we have constants $\eta \in (0, 1)$, $\delta \in (0, 1)$, $a \in (1/2, \infty)$, and $b_n \in (0, 1)$, where $b_n \rightarrow 0$ as $n \rightarrow \infty$. Then there exists a nonnegative and measurable real-valued function $\tilde{h}_n(y)$ such that $\text{Var}(\beta|x) \leq \tilde{h}_n(y)$ for all $y \in \mathbb{R}$. Moreover, $\tilde{h}_n(y) \rightarrow 1$ as $y \rightarrow \infty$ for any fixed $b_n \in (0, 1)$, and $\tilde{h}_n(y)$ satisfies the following:*

For any $d > 1$, $h_n(\cdot)$ satisfies

$$\lim_{n \rightarrow \infty} \sup_{|y| > \sqrt{2\rho \log(\frac{1}{b_n})}} \tilde{h}_n(y) = 1 \text{ for any } \rho > d. \quad (\text{B.28})$$

Proof of Lemma B.5. We use the representation of $\text{Var}(\beta|x)$ given in (B.26). It is clear that $\frac{T(y)}{y} - (T(y) - y)^2$ can be bounded above by $\tilde{h}_1(y) = 1$ for all $y \in \mathbb{R}$. To bound the last term in (B.26), fix $\eta \in (0, 1)$ and $\delta \in (0, 1)$, and split this term into the sum,

$$y^2 \frac{\int_0^\eta \kappa^{a+3/2} (1-\kappa)^{b_n-1} e^{-\kappa y^2/2} d\kappa}{\int_0^1 \kappa^{a-1/2} (1-\kappa)^{b_n-1} e^{-\kappa y^2/2} d\kappa} + y^2 \frac{\int_\eta^1 \kappa^{a+3/2} (1-\kappa)^{b_n-1} e^{-\kappa y^2/2} d\kappa}{\int_0^1 \kappa^{a-1/2} (1-\kappa)^{b_n-1} e^{-\kappa y^2/2} d\kappa}. \quad (\text{B.29})$$

Following the same techniques as in Lemma B.3 to bound each term in the sum above, we can show that there exists a real-valued function $\tilde{h}_2(y)$ for which (B.29) is uniformly bounded above by $\tilde{h}_2(y)$ for all $y \in \mathbb{R}$ and for which $\tilde{h}_2(y) \rightarrow 0$ as $y \rightarrow \infty$ for any fixed n . Moreover, by mimicking the

proof for Lemma B.3, it can similarly be shown that, for any $d > 1$, this function $\tilde{h}_2(y)$ satisfies

$$\lim_{n \rightarrow \infty} \sup_{|y| > \sqrt{2\rho \log(\frac{1}{b_n})}} \tilde{h}_2(y) = 0 \text{ for any } \rho > d.$$

Therefore, letting $\tilde{h}_n(y) = \tilde{h}_1(y) + \tilde{h}_2(y) = 1 + \tilde{h}_2(y)$, the lemma is proven. \square

Lemma B.6. *Define $J_n(y)$ as follows:*

$$J_n(y) = y^2 \frac{\int_0^1 \kappa^{a-1/2} (1-\kappa)^{b_n+1} e^{-\kappa y^2/2} d\kappa}{\int_0^1 \kappa^{a-1/2} (1-\kappa)^{b_n-1} e^{-\kappa y^2/2} d\kappa}. \quad (\text{B.30})$$

Suppose that $a \in (1/2, \infty)$ is fixed and $b_n \in (0, 1)$ for all n . Then we have the following upper bound for $J_n(x)$:

$$J_n(y) \leq b_n e^{y^2/2} \left(\frac{\Gamma(a + b_n + 1/2)}{\Gamma(a + 1/2)\Gamma(b_n + 1)} \right). \quad (\text{B.31})$$

Proof of Lemma B.6. We have

$$\begin{aligned} J_n(y) &= y^2 \frac{\int_0^1 \kappa^{a-1/2} (1-\kappa)^{b_n+1} e^{-\kappa y^2/2} d\kappa}{\int_0^1 \kappa^{a-1/2} (1-\kappa)^{b_n-1} e^{-\kappa y^2/2} d\kappa} \\ &\leq y^2 e^{y^2/2} \frac{\int_0^1 \kappa^{a-1/2} (1-\kappa)^{b_n+1} e^{-\kappa y^2/2} d\kappa}{\int_0^1 \kappa^{a-1/2} (1-\kappa)^{b_n-1} d\kappa} \\ &= y^2 e^{y^2/2} \frac{\Gamma(a + b_n + 1/2)}{\Gamma(a + 1/2)\Gamma(b_n)} \int_0^1 \kappa^{a-1/2} (1-\kappa)^{b_n+1} e^{-\kappa y^2/2} d\kappa \\ &= e^{y^2/2} \frac{\Gamma(a + b_n + 1/2)}{\Gamma(a + 1/2)\Gamma(b_n)} \int_0^{y^2} \left(\frac{t}{y^2}\right)^{a-1/2} \left(1 - \frac{t}{y^2}\right)^{b_n+1} e^{-t/2} dt, \end{aligned} \quad (\text{B.32})$$

where we used a transformation of variables $t = \kappa y^2$ in the last equality. For $0 < t < y^2$, we have $0 < \left(1 - \frac{t}{y^2}\right) < 1$, and since $b_n \in (0, 1)$ for all n , we have $\left(1 - \frac{t}{y^2}\right)^{b_n+1} < 1$ for all n . Therefore, from (B.32), we may further bound $J_n(y)$ from above as

$$J_n(y) \leq e^{y^2/2} (y^2)^{1/2-a} \frac{\Gamma(a + b_n + 1/2)}{\Gamma(a + 1/2)\Gamma(b_n)} \int_0^{y^2} t^{a-1/2} e^{-t/2} dt$$

$$\begin{aligned}
&\leq e^{y^2/2} \frac{\Gamma(a + b_n + 1/2)}{\Gamma(a + 1/2)\Gamma(b_n)} \int_0^{y^2} e^{-t/2} dt \\
&\leq 2e^{y^2/2} \frac{\Gamma(a + b_n + 1/2)}{\Gamma(a + 1/2)\Gamma(b_n)} \\
&= 2b_n e^{y^2/2} \left(\frac{\Gamma(a + b_n + 1/2)}{\Gamma(a + 1/2)\Gamma(b_n + 1)} \right),
\end{aligned}$$

where we used the fact that $a \in (1/2, \infty)$ and thus, $t^{a-1/2}$ is increasing in $t \in (0, y^2)$ for the second inequality, and the fact that $\Gamma(b_n + 1) = b_n \Gamma(b_n)$ for the last equality. \square

Lemmas B.2-B.6 are crucial for proving the next two lemmas, which provide asymptotic upper bounds on the mean squared error (MSE) for the posterior mean under the NBP $_n$ prior (4.13) and the posterior variance under (4.13). These lemmas will ultimately allow us to provide sufficient conditions under which the posterior mean and posterior distribution under the NBP $_n$ prior contract at minimax rates.

Lemma B.7. *Suppose $\mathbf{y} \sim \mathcal{N}(\boldsymbol{\beta}_0, \mathbf{I}_n)$, where $\boldsymbol{\beta}_0 \in \ell_0[q_n]$. Let $T(\mathbf{y})$ denote the posterior mean vector under (4.13). If $a \in (1/2, \infty)$, $b_n \in (0, 1)$ with $b_n \rightarrow 0$ as $n \rightarrow \infty$, the MSE satisfies*

$$\sup_{\boldsymbol{\beta}_0 \in \ell_0[q_n]} \mathbb{E}_{\boldsymbol{\beta}_0} \|T(\mathbf{y}) - \boldsymbol{\beta}_0\|^2 \lesssim q_n \log\left(\frac{1}{b_n}\right) + (n - q_n)b_n \sqrt{\log\left(\frac{1}{b_n}\right)},$$

provided that $q_n \rightarrow \infty$ and $q_n = o(n)$ as $n \rightarrow \infty$.

Proof of Lemma B.7. Define $\tilde{q}_n = \#\{i : \beta_{0i} \neq 0\}$. We split the MSE,

$$\mathbb{E}_{\boldsymbol{\beta}_0} \|T(\mathbf{y}) - \boldsymbol{\beta}_0\|^2 = \sum_{i=1}^n \mathbb{E}_{\beta_{0i}} (T(y_i) - \beta_{0i})^2$$

as

$$\sum_{i=1}^n \mathbb{E}_{\beta_{0i}} (T(y_i) - \beta_{0i})^2 = \sum_{i:\beta_{0i} \neq 0} \mathbb{E}_{\beta_{0i}} (T(y_i) - \beta_{0i})^2 + \sum_{i:\beta_{0i} = 0} \mathbb{E}_{\beta_{0i}} (T(X_i) - \beta_{0i})^2. \quad (\text{B.33})$$

We consider the nonzero means and the zero means separately.

Nonzero means: For $\beta_{0i} \neq 0$, using the Cauchy-Schwartz inequality and the fact that $\mathbb{E}_{\beta_{0i}} (y_i - \beta_{0i})^2 = 1$, we get

$$\mathbb{E}_{\beta_{0i}} (T(y_i) - \beta_{0i})^2 = \mathbb{E}_{\beta_{0i}} (T(y_i) - y_i + y_i - \beta_{0i})^2$$

$$\begin{aligned}
&= \mathbb{E}_{\beta_{0i}}(T(y_i) - y_i)^2 + \mathbb{E}_{\beta_{0i}}(y_i - \beta_{0i})^2 + 2\mathbb{E}_{\beta_{0i}}(T(y_i) - y_i)(y_i - \beta_{0i}) \\
&\leq \mathbb{E}_{\beta_{0i}}(T(y_i) - y_i)^2 + 1 + 2\sqrt{\mathbb{E}_{\beta_{0i}}(T(y_i) - y_i)^2}\sqrt{\mathbb{E}_{\beta_{0i}}(y_i - \beta_{0i})^2} \\
&= \left[\sqrt{\mathbb{E}_{\beta_{0i}}(T(y_i) - y_i)^2 + 1} \right]^2.
\end{aligned} \tag{B.34}$$

We now define

$$\zeta_n = \sqrt{2 \log \left(\frac{1}{b_n} \right)}. \tag{B.35}$$

Let us fix any $d > 2$ and choose any $\rho > d$. Then, using Lemma B.3, there exists a non-negative real-valued function $h_n(\cdot)$, depending on d such that

$$|T_n(y) - y| \leq h_n(y) \text{ for all } y \in \mathbb{R}, \tag{B.36}$$

and

$$\lim_{n \rightarrow \infty} \sup_{|y| > \rho \zeta_n} h_n(y) = 0. \tag{B.37}$$

Using the fact that $(T(y_i) - y_i)^2 \leq y_i^2$, together with (B.37), we obtain

$$\begin{aligned}
\mathbb{E}_{\beta_{0i}}(T(y_i) - y_i)^2 &= \mathbb{E}_{\beta_{0i}}[(T(y_i) - y_i)^2 \mathbf{1}\{|X_i| \leq \rho \zeta_n\}] \\
&\quad + \mathbb{E}_{\beta_{0i}}[T(y_i - y_i)^2 \mathbf{1}\{|y_i| > \rho \zeta_n\}] \\
&\leq \rho^2 \zeta_n^2 + \left(\sup_{|y| > \rho \zeta_n} h_n(y) \right)^2.
\end{aligned} \tag{B.38}$$

Using (B.37) and the fact that $\zeta_n \rightarrow \infty$ as $n \rightarrow \infty$ by (B.35), it follows that

$$\left(\sup_{|y| > \rho \zeta_n} h_n(y) \right)^2 = o(\zeta_n^2) \text{ as } n \rightarrow \infty. \tag{B.39}$$

By combining (B.38) and (B.39), we get

$$\mathbb{E}_{\beta_{0i}}(T(y_i) - y_i)^2 \leq \rho^2 \zeta_n^2 (1 + o(1)) \text{ as } n \rightarrow \infty. \tag{B.40}$$

Noting that (B.40) holds uniformly for any i such that $\beta_{0i} \neq 0$, we combine (B.34), (B.35), and (B.40) to conclude that

$$\sum_{i: \beta_{0i} \neq 0} \mathbb{E}_{\beta_{0i}}(T(y_i) - \beta_{0i})^2 \lesssim \tilde{q}_n \log \left(\frac{1}{b_n} \right), \text{ as } n \rightarrow \infty, \tag{B.41}$$

Zero means: For $\beta_{0i} = 0$, the corresponding MSE can be split as follows:

$$\mathbb{E}_0 T(y_i)^2 = \mathbb{E}_0[T(y_i)^2 \mathbf{1}\{|y_i| \leq \zeta_n\}] + \mathbb{E}_0[T(y_i)^2 \mathbf{1}\{|y_i| > \zeta_n\}], \quad (\text{B.42})$$

where ζ_n is as in (B.35). Using (B.15) from Lemma B.2, we have

$$\begin{aligned} \mathbb{E}_0[T(y_i)^2 \mathbf{1}\{|y_i| \leq \zeta_n\}] &\leq \left(\frac{b_n}{a + b_n + 1/2} \right)^2 \int_{-\zeta_n}^{\zeta_n} y^2 e^{y^2/2} dy \\ &\leq \frac{b_n^2}{a^2} \int_{-\zeta_n}^{\zeta_n} y^2 e^{y^2/2} dy \\ &= \frac{2b_n^2}{a^2} \int_0^{\zeta_n} y^2 e^{y^2/2} dy \\ &\leq \frac{2b_n^2}{a} (\zeta_n e^{\zeta_n^2/2}) \\ &\lesssim b_n \sqrt{\log\left(\frac{1}{b_n}\right)}, \end{aligned} \quad (\text{B.43})$$

where we use the integration by parts for the third inequality.

Now, using the fact that $|T(y)| \leq |y|$ for all $y \in \mathbb{R}$,

$$\begin{aligned} \mathbb{E}_0[T(y_i)^2 \mathbf{1}\{|y_i| > \zeta_n\}] &\leq 2 \int_{\zeta_n}^{\infty} y^2 \phi(y) dy \\ &\leq 2\zeta_n \phi(\zeta_n) + \frac{2\phi(\zeta_n)}{\zeta_n} \\ &= \sqrt{\frac{2}{\pi}} \zeta_n \left(e^{-\zeta_n^2/2} + o(1) \right) \\ &\lesssim b_n \sqrt{\log\left(\frac{1}{b_n}\right)}, \end{aligned} \quad (\text{B.44})$$

where we used the identity $y^2 \phi(y) = \phi(y) - \frac{d}{dy}[y\phi(y)]$ for the first equality and Mill's ratio, $1 - \Phi(y) \leq \frac{\phi(y)}{y}$ for all $y > 0$, in the second inequality. Combining (B.43)-(B.44), we have that

$$\sum_{i:\beta_{0i}=0} \mathbb{E}_{\beta_{0i}} T(y_i)^2 \lesssim (n - \tilde{q}_n) b_n \sqrt{\log\left(\frac{1}{b_n}\right)}. \quad (\text{B.45})$$

From (B.33), (B.41) and (B.45), it immediately follows that

$$\mathbb{E}_{\beta_0} \|T(\mathbf{y}) - \beta_0\|^2 = \sum_{i=1}^n \mathbb{E}_{\beta_{0i}} (T(y_i) - \beta_{0i})^2$$

$$\lesssim \tilde{q}_n \log\left(\frac{1}{b_n}\right) + (n - \tilde{q}_n)b_n \sqrt{\log\left(\frac{1}{b_n}\right)}.$$

The required result now follows by observing that $\tilde{q}_n \leq q_n$ and $q_n = o(n)$ and then taking the supremum over all $\beta_0 \in \ell_0[q_n]$. This completes the proof of Lemma B.7. \square

Lemma B.8. *Suppose $\mathbf{y} \sim \mathcal{N}(\beta_0, \mathbf{I}_n)$, where $\beta_0 \in \ell_0[q_n]$. Under prior (4.13) and assumptions that $a \in (1/2, \infty)$ and $b_n \in (0, 1)$ with $b_n \rightarrow 0$ as $n \rightarrow \infty$, the total posterior variance satisfies*

$$\sup_{\beta_0 \in \ell_0[q_n]} \mathbb{E}_{\beta_0} \sum_{i=1}^n \text{Var}(\beta_{0i}|y_i) \lesssim q_n \log\left(\frac{1}{b_n}\right) + (n - q_n)b_n \sqrt{\log\left(\frac{1}{b_n}\right)},$$

provided that $q_n \rightarrow \infty$ and $q_n = o(n)$ as $n \rightarrow \infty$.

Proof of Lemma B.8. Define $\tilde{q}_n = \#\{i : \beta_{0i} \neq 0\}$. We decompose the total variance as

$$\mathbb{E}_{\beta_0} \sum_{i=1}^n \text{Var}(\beta_{0i}|y_i) = \sum_{i:\beta_{0i} \neq 0} \mathbb{E}_{\beta_{0i}} \text{Var}(\beta_{0i}|y_i) + \sum_{i:\beta_{0i}=0} \mathbb{E}_{\beta_{0i}} \text{Var}(\beta_{0i}|y_i), \quad (\text{B.46})$$

and consider the nonzero means and zero means separately.

Nonzero means: Fix $d > 1$ and choose any $\rho > d$, and let ζ_n be defined as in (B.35). For $\beta_{0i} \neq 0$, we have from (B.28) in Lemma B.5 that

$$\mathbb{E}_{\beta_{0i}} [\text{Var}(\beta_i|y_i) 1\{|y_i| > \rho\zeta_n\}] \lesssim 1. \quad (\text{B.47})$$

Moreover, Lemma B.4 shows that $\text{Var}(\beta|y) \leq 1 + y^2$ for any $y \in \mathbb{R}$, and so we must also have that as $n \rightarrow \infty$,

$$\mathbb{E}_{\beta_{0i}} [\text{Var}(\beta_i|y_i) 1\{|y_i| \leq \rho\zeta_n\}] \lesssim \zeta_n^2. \quad (\text{B.48})$$

Combining (B.47) and (B.48), we have that, as $n \rightarrow \infty$,

$$\mathbb{E}_{\beta_{0i}} \text{Var}(\beta_i|X_i) \lesssim 1 + \zeta_n^2,$$

and thus, for all i such that $\beta_i \neq 0$,

$$\sum_{i:\beta_{0i} \neq 0} \mathbb{E}_{\beta_{0i}} \text{Var}(\beta_{0i}|X_i) \lesssim \tilde{q}_n (1 + \zeta_n^2) \lesssim \tilde{q}_n \log\left(\frac{1}{b_n}\right). \quad (\text{B.49})$$

Zero means: For $\beta_{0i} = 0$, we use same ζ_n that we used for the nonzero means. We have from Lemma B.4 that $\text{Var}(\beta|y) \leq 1 + y^2$. Using the identity $y^2\phi(y) = \phi(y) - \frac{d}{dy}[y\phi(y)]$ for $y \in \mathbb{R}$, we obtain that as $n \rightarrow \infty$,

$$\begin{aligned} \mathbb{E}_0 [\text{Var}(\beta_i|y_i)1\{|y_i| > \zeta_n\}] &\leq 2 \int_{\zeta_n}^{\infty} (1 + y^2) \frac{1}{\sqrt{2\pi}} e^{-y^2/2} dx \\ &\lesssim \frac{b_n}{\zeta_n} + \zeta_n b_n \\ &\lesssim b_n \sqrt{\log\left(\frac{1}{b_n}\right)}. \end{aligned} \quad (\text{B.50})$$

Next, we consider $|y_i| \leq \zeta_n$. We have by (B.27) in Lemma B.4 that $\text{Var}(\beta|x) \leq \frac{T(y)}{y} + J_n(y)$, where $J_n(y)$ is the last term in (B.27). Lemma B.6 gives an upper bound (B.31) on $J_n(y)$. Since $a \in (1/2, \infty)$ is fixed and $b_n \in (0, 1)$ with $b_n \rightarrow 0$ as $n \rightarrow \infty$, the term in parentheses in (B.31) can be uniformly bounded above by a constant (which depends on a). Therefore, we have by Lemma B.6 that $J_n(y) \lesssim b_n$. Moreover, $\frac{T(y)}{y} = \mathbb{E}(1 - \kappa|y)$, and it is clear from (B.15) in Lemma B.2 that $\mathbb{E}(1 - \kappa|y) \lesssim b_n$. Altogether, we have that as $n \rightarrow \infty$,

$$\begin{aligned} \mathbb{E}_0 [\text{Var}(\beta_i|y_i)1\{|y_i| \leq \zeta_n\}] &\lesssim \zeta_n b_n \\ &\lesssim b_n \sqrt{\log\left(\frac{1}{b_n}\right)} \end{aligned} \quad (\text{B.51})$$

Combining (B.50) and (B.51), it follows that as $n \rightarrow \infty$,

$$\mathbb{E}_0 \text{Var}(\theta_i|y_i) \lesssim b_n \sqrt{\log\left(\frac{1}{b_n}\right)},$$

and consequently,

$$\sum_{i:\beta_{0i}=0} \mathbb{E}_{\beta_{0i}} \text{Var}(\beta_{0i}|y_i) \lesssim (n - \tilde{q}_n) b_n \sqrt{\log\left(\frac{1}{b_n}\right)}. \quad (\text{B.52})$$

Combining (B.46), (B.49), and (B.52), it follows that as $n \rightarrow \infty$,

$$\mathbb{E}_{\beta_0} \sum_{i=1}^n \text{Var}(\beta_i|y_i) \lesssim \tilde{q}_n \log\left(\frac{1}{b_n}\right) + (n - \tilde{q}_n) b_n \sqrt{\log\left(\frac{1}{b_n}\right)}$$

The required result now follows by observing that $\tilde{q}_n \leq q_n$ and $q_n = o(n)$ and then taking the supremum over all $\theta_0 \in \ell_0[q_n]$. This completes the proof of Lemma B.8. \square

Having proven Lemmas B.7 and B.8, we are now ready to prove Theorem 4.2, which shows that the NBP_n (4.13) model achieves the minimax posterior contraction rate under the normal means model (4.9).

Proof of Theorem 4.2. Suppose that q_n is known, and that we set $a \in (1/2, \infty)$ and $b_n = (q_n/n)^\alpha$, where $\alpha \geq 1$. Then by Lemma B.7, we immediately have

$$\sup_{\beta_0 \in \ell_0[q_n]} \mathbb{E}_{\beta_0} \|\widehat{\beta} - \beta_0\|^2 \lesssim q_n \log \left(\frac{n}{q_n} \right),$$

where $\widehat{\beta}$ is the posterior mean. This proves (4.15). To prove that

$$\sup_{\beta_0 \in \ell_0[q_n]} \mathbb{E}_{\beta_0} \Pi \left(\|\beta - \beta_0\|_2^2 > M_n q_n \log \left(\frac{n}{q_n} \right) \mid \mathbf{y}_n \right) \rightarrow 0,$$

we use a straightforward application of Markov's inequality, combined with the results of Lemmas B.7 and B.8. Thus, (4.14) is also proven. \square

References

- [1] Armagan, A., Clyde, M., and Dunson, D. B. (2011). Generalized beta mixtures of gaussians. In Shawe-taylor, J., Zemel, R., Bartlett, P., Pereira, F., and Weinberger, K., editors, *Advances in Neural Information Processing Systems 24*, pages 523–531.
- [2] Armagan, A., Dunson, D. B., and Lee, J. (2013). Generalized double pareto shrinkage. *Statistica Sinica*, 23 1:119–143.
- [3] Bai, R. and Ghosh, M. (2018). Large-scale multiple hypothesis testing with the normal-beta prime prior. *ArXiv pre-print arXiv: 1807.02421*.
- [4] Berger, J. (1980). A robust generalized bayes estimator and confidence region for a multivariate normal mean. *Ann. Statist.*, 8(4):716–761.
- [5] Bhadra, A., Datta, J., Polson, N. G., and Willard, B. (2017). The horseshoe+ estimator of ultra-sparse signals. *Bayesian Anal.*, 12(4):1105–1131.
- [6] Bhattacharya, A., Chakraborty, A., and Mallick, B. K. (2016). Fast sampling with gaussian scale mixture priors in high-dimensional regression. *Biometrika*, 103(4):985–991.

- [7] Bhattacharya, A., Pati, D., Pillai, N. S., and Dunson, D. B. (2015). Dirichlet–laplace priors for optimal shrinkage. *Journal of the American Statistical Association*, 110(512):1479–1490. PMID: 27019543.
- [8] Candes, E. and Tao, T. (2007). The dantzig selector: Statistical estimation when p is much larger than n . *Ann. Statist.*, 35(6):2313–2351.
- [9] Carvalho, C. M., Polson, N. G., and Scott, J. G. (2009). Handling sparsity via the horseshoe. In van Dyk, D. and Welling, M., editors, *Proceedings of the Twelfth International Conference on Artificial Intelligence and Statistics*, volume 5 of *Proceedings of Machine Learning Research*, pages 73–80, Hilton Clearwater Beach Resort, Clearwater Beach, Florida USA. PMLR.
- [10] Carvalho, C. M., Polson, N. G., and Scott, J. G. (2010). The horseshoe estimator for sparse signals. *Biometrika*, 97(2):465–480.
- [11] Casella, G. (2001). Empirical bayes gibbs sampling. *Biostatistics*, 2(4):485–500.
- [12] Datta, J. and Ghosh, J. K. (2013). Asymptotic properties of bayes risk for the horseshoe prior. *Bayesian Anal.*, 8(1):111–132.
- [13] Donoho, D. L., Johnstone, I. M., Hoch, J. C., and Stern, A. S. (1992). Maximum entropy and the nearly black object. *Journal of the Royal Statistical Society. Series B (Methodological)*, 54(1):41–81.
- [14] Fan, J. and Li, R. (2001). Variable selection via nonconcave penalized likelihood and its oracle properties. *Journal of the American Statistical Association*, 96(456):1348–1360.
- [15] George, E. and Foster, D. P. (2000). Calibration and empirical bayes variable selection. *Biometrika*, 87(4):731–747.
- [16] Ghosal, S., Ghosh, J. K., and van der Vaart, A. W. (2000). Convergence rates of posterior distributions. *Ann. Statist.*, 28(2):500–531.
- [17] Ghosh, P. and Chakrabarti, A. (2017). Asymptotic optimality of one-group shrinkage priors in sparse high-dimensional problems. Advance publication.
- [18] Ghosh, P., Tang, X., Ghosh, M., and Chakrabarti, A. (2016). Asymptotic properties of bayes risk of a general class of shrinkage priors in multiple hypothesis testing under sparsity. *Bayesian Anal.*, 11(3):753–796.

- [19] Griffin, J. E. and Brown, P. J. (2010). Inference with normal-gamma prior distributions in regression problems. *Bayesian Anal.*, 5(1):171–188.
- [20] Griffin, J. E. and Brown, P. J. (2013). Some priors for sparse regression modelling. *Bayesian Anal.*, 8(3):691–702.
- [21] Hahn, P. R. and Carvalho, C. M. (2015). Decoupling shrinkage and selection in bayesian linear models: A posterior summary perspective. *Journal of the American Statistical Association*, 110(509):435–448.
- [22] Johnstone, I. M. and Silverman, B. W. (2004). Needles and straw in haystacks: Empirical bayes estimates of possibly sparse sequences. *Ann. Statist.*, 32(4):1594–1649.
- [23] Leday, G. G. R., de Gunst, M. C. M., Kpogbezan, G. B., van der Vaart, A. W., van Wieringen, W. N., and van de Wiel, M. A. (2017). Gene network reconstruction using global-local shrinkage priors. *Ann. Appl. Stat.*, 11(1):41–68.
- [24] Park, T. and Casella, G. (2008). The bayesian lasso. *Journal of the American Statistical Association*, 103(482):681–686.
- [25] Piironen, J. and Vehtari, A. (2017a). On the Hyperprior Choice for the Global Shrinkage Parameter in the Horseshoe Prior. In Singh, A. and Zhu, J., editors, *Proceedings of the 20th International Conference on Artificial Intelligence and Statistics*, volume 54 of *Proceedings of Machine Learning Research*, pages 905–913, Fort Lauderdale, FL, USA. PMLR.
- [26] Piironen, J. and Vehtari, A. (2017b). Sparsity information and regularization in the horseshoe and other shrinkage priors. *Electron. J. Statist.*, 11(2):5018–5051.
- [27] Polson, N. G. and Scott, J. G. (2010). Shrink globally, act locally: Sparse bayesian regularization and prediction. *Bayesian Statistics*, 9:501–538.
- [28] Polson, N. G. and Scott, J. G. (2012). On the half-cauchy prior for a global scale parameter. *Bayesian Anal.*, 7(4):887–902.
- [29] Raskutti, G., Wainwright, M. J., and Yu, B. (2011). Minimax rates of estimation for high-dimensional linear regression over ell_q -balls. *IEEE Transactions on Information Theory*, 57(10):6976–6994.

- [30] Ročková, V. (2018). Bayesian estimation of sparse signals with a continuous spike-and-slab prior. *Ann. Statist.*, 46(1):401–437.
- [31] Ročková, V. and George, E. I. (2018). The spike-and-slab lasso. *Journal of the American Statistical Association*, 113(521):431–444.
- [32] Scheetz, T. E., Kim, K.-Y. A., Swiderski, R. E., Philp, A. R., Braun, T. A., Knudtson, K. L., Dorrance, A. M., DiBona, G. F., Huang, J., Casavant, T. L., Sheffield, V. C., and Stone, E. M. (2006). Regulation of gene expression in the mammalian eye and its relevance to eye disease. *Proceedings of the National Academy of Sciences*, 103(39):14429–14434.
- [33] Scott, J. G. and Berger, J. O. (2010). Bayes and empirical-bayes multiplicity adjustment in the variable-selection problem. *Ann. Statist.*, 38(5):2587–2619.
- [34] Song, Q. and Liang, F. (2017). Nearly optimal bayesian shrinkage for high dimensional regression. *ArXiv pre-print arXiv: 1712.08964*.
- [35] Strawderman, W. E. (1971). Proper bayes minimax estimators of the multivariate normal mean. *Ann. Math. Statist.*, 42(1):385–388.
- [36] Tibshirani, R. (1996). Regression shrinkage and selection via the lasso. *Journal of the Royal Statistical Society, Series B*, 58:267–288.
- [37] van der Pas, S., Salomond, J.-B., and Schmidt-Hieber, J. (2016). Conditions for posterior contraction in the sparse normal means problem. *Electron. J. Statist.*, 10(1):976–1000.
- [38] van der Pas, S., Szabó, B., and van der Vaart, A. (2017). Adaptive posterior contraction rates for the horseshoe. *Electron. J. Statist.*, 11(2):3196–3225.
- [39] van der Pas, S. L., Kleijn, B. J. K., and van der Vaart, A. W. (2014). The horseshoe estimator: Posterior concentration around nearly black vectors. *Electron. J. Statist.*, 8(2):2585–2618.
- [40] Xiang, D. and Jones, G. L. (2017). Bayesian Penalized Regression. *ArXiv pre-print arXiv: 1706.07767*.
- [41] Zhang, C.-H. (2010). Nearly unbiased variable selection under minimax concave penalty. *Ann. Statist.*, 38(2):894–942.

- [42] Zou, H. and Hastie, T. (2005). Regularization and variable selection via the elastic net. *Journal of the Royal Statistical Society: Series B (Statistical Methodology)*, 67(2):301–320.